



**Sudan University of Science and Technology**

**College of Engineering**

**Biomedical Engineering Department**



## **DESIGN OF TRI-STAR WHEEL ROBOT**

**تصميم آلية كهروميكانيكية باستخدام العجلة الثلاثية**

A thesis submitted in partial fulfillment of the requirements for the degree of BSc  
Biomedical Engineering

**By**

Dalia Abd-Elwahab Mohammed Khair Mahmoud

Maha Fath Alaleem Abd Alhaleem Ayed

Sara Tayeb Alassma Ahmed Mohammed

**Supervisor:**

Dr.Megdi Elnour Abdulrahman

**October 2017**

# **Dedication**

For all disabled who really need this creation and to everyone helped us everywhere and at each level

# **Acknowledgement**

First of all we thank Allah

We would like to thank all at mechanical engineering department at workshops

Dr. Gaffer Abd-alhameed

Eng. Hammed abdallah Abbakar

Eng. Mohammed abbas

And all who helped us. May Allah bless you all.

We deeply beholden to our supervisor Dr. Megdi Alnour for all the support and guidance he provided throughout our project.

## **Abstract**

Stair climber as a mean of transport tool plays an important role in the life of those people who are old or disabled the stair climber can easily access many places include stairs.

This project use the planetary (tri-star) wheels mechanism to actualize the motion on stairs to design a base with optimum combination of dimensions and material with parameters set for acceptable motion.

The main objective of this project is to design and develop mechanism that make the disable person climb stairs without assistant. Solid work 2016 software is used to create a 3D model and analysis it to obtain the impact of the external forces act on the main items of the design and the deformation result from them.

The main parameters collected and provided in the 3D model. They involved the dimensions of the stair, the holder and its component which are: height of the stair is 17cm, width of stairs is 30cm, radius of regular wheel is 24cm, distance between the center of Tri-Star wheel and the center of its wheel is 22cm and thickness of holders is 6cm that fix the wheel on its place on Tri-Star wheel.

Depending on the result obtained from analysis of design, it was improved and modified to give acceptable performance.

## المستخلص

متسلق السلالم كوسيلة نقل يلعب دور مهم في حياة كبار السن وذوي الإعاقة البدنية حيث يساعدهم في الوصول لجميع الأماكن المتضمنة للسلالم.

موضوع البحث يتناول تصميم وسيلة النقل المذكورة باستخدام منظومة العجلة الثلاثية كوسيلة للحركة على السلالم وذلك بالإستعانة بالأبعاد القياسية ومجموعة من المعاملات للحصول على الحركة المطلوبة.

الهدف الأساسي من البحث هو تصميم وتطوير آلية تمكن المستخدم من الحركة على السلالم بدون الحاجة لتدخل مساعدات خارجية وذلك بعمل تصميم ثلاثي الأبعاد وتطبيق وتحليل القوى الخارجية المؤثرة على الأجزاء الرئيسية من التصميم والتحصل على نتائج التشوه الناتج وذلك بإستخدام برنامج (SOLIDWORK 2016).

تم جمع المعاملات الأساسية وتضمينها في النموذج الثلاثي الأبعاد والتي تضمن مقاسات السلم و هي ارتفاع السلم (17سم) و عرض السلم (30سم) ، أبعاد حامل العجلات وهي المسافة ما بين المركزين مركز المنظومة و مركز العجلة (22سم) و عرضه (6سم) و قطر العجلة (24سم).

اعتمادا على النتائج المتحصل عليها من التحليل تم تعديل التصميم و تحسينه .

# Table of content

Dedication .....	I
Acknowledgement .....	II
Abstract.....	III
المستخلص.....	IV
Table of content.....	V
List of Figures .....	VIII
List of Tables .....	X
Chapter One Introduction and Background.....	1
1.1 Background .....	1
1.2 Problem Statement.....	1
1.3 Objectives of the research .....	2
1.3.1 General objective .....	2
1.3.2 Specific objective .....	2
1.4 Methodology.....	2
1.5 The Structure of the Thesis.....	2
Chapter Two Literature Review .....	4
2.1 Previous Studies.....	4
2.2 Component design .....	10
2.2.1 Transmutation system design .....	10
2.2.2 Transmitting torque to and from shafts .....	11
2.2.3 Shaft bearings .....	12
Chapter Three Theoretical Background .....	17
3.1 Concept Development .....	17
3.1.1 Design Concept .....	17
3.1.2 Procedure of movement .....	17
3.1.3 Process for Climbing Stairs.....	18
3.2 Determination Of The Basic Parameters .....	18
3.2.1 Tri-Star Wheel holder.....	19
3.2.2 Radius of regular Wheel.....	20
3.2.3 Dimension of key seat.....	21
3.3 Transmission system .....	21

3.3.1 Working principle for the transmission system .....	21
3.3.2 Gear Selection .....	22
3.4 Bearing calculations .....	24
3.4.1 Load applied to the bearing by power transmission .....	24
3.4.2 Gear transmission .....	24
3.5 Motor Selection .....	25
3.5.1 Speed determination .....	25
3.5.2 Torque determination.....	25
3.5.3 Power checked.....	26
Chapter Four Design .....	27
4.1 Introduction .....	27
4.2 Methodology.....	27
4.3 Initial design Structure calculation .....	28
4.3.1 Determine baseline model dimension.....	28
4.3.2 Gear Selection.....	29
4.3.3 Simulation Study .....	31
4.4 Improved design.....	31
4.4.1 Holder.....	32
4.4.2 Shaft .....	32
4.4.3 Key seat .....	33
4.4.4 Wheels .....	33
4.4.5 Gears .....	34
4.4.6 Force estimation .....	35
4.4.7 Bearing selection.....	35
4.5 Motor selection.....	36
4.5.1 Speed determination .....	36
4.5.2 Torque determination.....	37
4.5.3 Powered checked.....	37
4.6 Shaft analysis.....	37
4.6.1 Normal stress .....	38
4.6.2 Torsion shear stress .....	38
4.6.3 Load at the gear pitch circle.....	39
4.6.4 Shear stress .....	39
4.6.5 Bending stresses .....	39

4.6.6 Twisting moment .....	43
4.6.7 Combined maximum shear stress.....	43
4.6.8 Maximum normal stress .....	43
4.6.9 Analysis of stress point critical section .....	44
4.7 Material selection .....	46
4.7.1 Frame and body holder material .....	47
4.7.2 Type of Wheel/Tires Material .....	47
4.7.3 Shaft materials .....	48
Chapter Five Results and Discussion.....	49
5.1 Introduction .....	49
5.2 Tri-wheel holder system analysis.....	49
5.2.1 Material of holder .....	49
5.2.2 Von misses stress .....	50
5.2.3 Von-misses strain .....	53
5.2.4 Displacement .....	56
5.2.5 Deformation.....	59
5.3 Final Design .....	62
5.4 Discussion.....	66
Chapter Six Conclusions and Recommendations.....	68
6.1 Conclusions .....	68
6.2 Recommendation.....	68
References .....	
Appendix A.....	
Appendix B .....	



## List of Figures

Figure No.:	Title	Page No.
Figure 2.1:	the legged architecture stair climber .....	5
Figure 2.2:	tracked robotic mechanism.....	5
Figure 2.3:	customized climbing wheelchair .....	6
Figure 2.4:	Lawn and Shiatsu design .....	7
Figure 2.5:	Pyra-Aid™, a design .....	7
Figure 2.6:	Sandeep H.Deshmukh Stair Climbing Transporters (SCT) .....	8
Figure 2.7:	track-wheel hybrid locomotion .....	8
Figure 2.8:	wheeled mobility design.....	9
Figure 2.9:	an ergonomically electric wheelchair with climbing stair functionality ....	10
Figure 2.10	self propelled wheel chair for climbing stairs .....	10
Figure 2.11:	key seat .....	12
Figure 2.13:	load type .....	15
Figure 3.1:	tri-star wheel structure.....	17
Figure 3.2:	Process for Climbing Stairs [21] .....	18
Figure 3.3:	Different type of stairs [22] .....	19
Figure 3.4:	an equilateral triangle (R) and radius of the wheel (r) .....	20
Figure 3.5:	(a) Minimum radius of regular wheel, (b) Maximum radius of regular wheel .....	21
Figure 3.6:	key seat dimensions.....	21
Figure 3.7:	Working principle for the transmission system.....	22
Figure 3.8:	Gear specifications .....	22
Figure 4.1:	flow chart describing systematic procedures for methodology.....	27

Figure 4.2:	The dimension of holder at solidwork.....	28
Figure 4.3:	the wheel.....	29
Figure 4.4:	The gears inside of the planetary wheels.....	30
Figure 4.5:	(a) manual simulation, (b) software simulation.....	31
Figure 4.6:	The holder.....	32
Figure 4.7:	Shaft with The location of support bearing is shown schematically. There are two key seat for fixing gear (on lift-side) and wheel (on the right-side) with the shaft. ....	32
Figure 4.8:	the wheel dimension .....	34
Figure 4.9:	gear with key seat .....	34
Figure 4.10:	middle gear .....	34
Figure 5.1:	Final shaft .....	62
Figure 5.2:	holder.....	62
Figure 5.3:	gear with key seat .....	63
Figure 5.4:	middle gear .....	63
Figure 5.5:	gear's key seat .....	63
Figure 5.6:	wheel's key seat.....	64
Figure 5.7:	middle shaft .....	64
Figure 5.8:	wheel .....	64
Figure 5.9:	final system design .....	65
Figure 5.10 :	tri star wheel design.....	65
Figure 5.11:	shaft stress points.....	66
Figure 5.12:	Max stress, strain and displacement for the 3 material.....	67

## List of Tables

Table No.:	Title	Page No.
Table 2.1:	power transmission system .....	11
Table 2.2:	ways for transmitting torque to and from shaft .....	11
Table 2-3 :	types of rolling bearing.....	13
Table 3.1:	Different type of stairs .....	19
Table 4.1:	gear specification .....	30
Table 4.2:	Various Wheel Materials and their Coefficient of friction.....	48
Table 5.1:	Max stress, strain and displacement of aluminium.....	49
Table 5.2:	Max stress, strain and displacement of stainless steel .....	49
Table 5.3:	Max stress, strain and displacement of mild steel .....	50
Table 5.4:	Von misses stress distribution .....	50
Table 5.5:	Von-misses strain distribution .....	53
Table 5.6:	Displacement distribution.....	56
Table 5.7:	The Resultant Deformation.....	59

# **Chapter One**

## **Introduction and Background**

### **1.1 Background**

Since the beginning of mankind, he has been improving himself in science and technology to overcome his difficulties and reach & improvise his comfort levels. There are 650 million people which are about 10% of the global population are disabled in the 1970s, and now the number has increased to 15% and it's on rise [1].

In the field of providing mobility for the elderly and disabled, the aspect of dealing with stairs continues largely unresolved. Stair climber as a mean of transport tool plays an important role in the life of those people who are old or disabled that stair climber can easily access many places include stairs.

This project deals with the development of a stair climbing robot with Tri-star wheels. The main technical topics have been discussed in this project are; mathematical modeling, simulation and material selection.

The robot uses Tri-star wheels, the planetary (tri-star) wheels mechanism that follow the rotation of the gears of the transmission system powered by high torque and low speed DC motor supplied by battery, therefore enabling the robot to climb stairs by rotating the Tri-star assembly and to move on flat area.

Structures and material used in robot must be able to carry load and climb stair easily and efficiently. The design structure and Stress analyses of the robot are carried out using SOLIDWORK 2016 to find how applied force will affect the material and design overall.

### **1.2 Problem Statement**

In cities it's difficult to find buildings without stairs which increase the suffering of disable people making them indeed need assistant every move which decrease their chances to live normal activities. At the other side it is not convenient and also financially not easy to fit

electric lifts everywhere. Therefore stair act as a repetitive obstacle for disabled restrict their ability to move without assistant.

## **1.3 Objectives of the research**

### **1.3.1 General objective**

The main objective of this project is to design and development mechanism that make the disable person climb stairs without assistant and select a proper material.

### **1.3.2 Specific objective**

In order to achieve the main objective we have to complete the following objective

1. Determine and calculate basic parameters of the design
2. Create 3-D *model* of the design using computer-aided-design system (SOLIDWORK).
3. Analysis forces applied on the design.
4. Select proper materials for all parts of design.
5. Stress analysis and chosen material by using solid work 2016
6. Modify and optimization design

## **1.4 Methodology**

At first information's from different papers, catalogs and solid designs were used to produce the measures of the suggested design, and then the mathematical calculations of the applied and determined forces were done and acquired in the suggested design theoretically. From the previously collected information the proper materials were determined and late after selected based on the analysis values resulted from the created 3-D model of the design and the simulation acquired in solid works.

## **1.5 The Structure of the Thesis**

This thesis focuses on the development of stair-climbing mechanisms. Chapter one introduction and background outlined of thesis, what's the problem need to be solved and objectives, Chapter two Literature review - provide the background of thesis and theoretical information about early works and the comparison of designs component. Chapter three theoretical backgrounds - contain mathematical equations and theories used in design. Chapter four design - this chapter describes the initial design, the mechanism, components dimension calculation, in addition to design analysis and design specification which meet the main objectives. Chapter five result and Discussions - -presents the result of analysis of

forces, material and final design and discusses if the objectives have been met. Chapter six conclusions- this chapter provide final summary for this project.

# Chapter Two

## Literature Review

### 2.1 Previous Studies

Stair climbing mechanism had been the point of investigation in many researches in the past decades. Scientist and researchers seek to provide the most comfortable situation for disabled to have a smooth and safe stair climbing and they sort of divided either to create a standalone device or an assistive device connected to stairs. Ultimately their efforts presented bio robots ,an engineering marvel, that was able to hold mass of human being and travel over obstacles ,staircase and in flat grounds. A number of robots had been built, such as quadruped and hexapod robots. Although these robots can climb stairs and traverse obstacles, they do not have smooth motion on flat surfaces, which is due to the motion of their legs [2]. Ghani ET. Al. investigate the control of a stair climbing wheelchair used for indoor purposes [3] .this research is presenting a development in the mechanism of stair climbing. The mechanism is based on switching both back and front wheels with tri wheels using gear system and motors to provide motion and microchips to provide assistant less control .however according to different researches the stair climbing robots can be categorized to wheeled ,legged and traced robots [2]. Figliolini and Ceccarelli presented a type of the legged architecture shown in figure 2.1 in the form of the bipedal robot EP-WAR2 that used electro pneumatic actuators and suction cups for locomotion. The operation was built upon putting the machine in an open-loop control algorithm. The main limitation of the approach is that operating in a different staircase necessitates manual recalibration [4].



**Figure 2.1: the legged architecture stair climber**

Tracked robots have a larger ground contact surface than wheeled vehicles and are more stable than bipeds due to their low center of gravity. Liu et al. presented a tracked robotic mechanism as shown in Figure using the fundamental dynamics of the stair-climbing process and the analysis of different phases of riser climbing, nose crossing, nose line climbing and the effects of grouser bars or cleats. The analysis was limited to 2D and slippage, shocks and intermittent loss of track-surface contact which is commonly encountered during stair climbing were neglected [5].



**Figure 2.2: tracked robotic mechanism**

Shashank Shekhar Sahoo, Himank Kinkar proposed customized climbing wheelchair shown in figure 2.3 consists of various mechanical and electronic components [6].

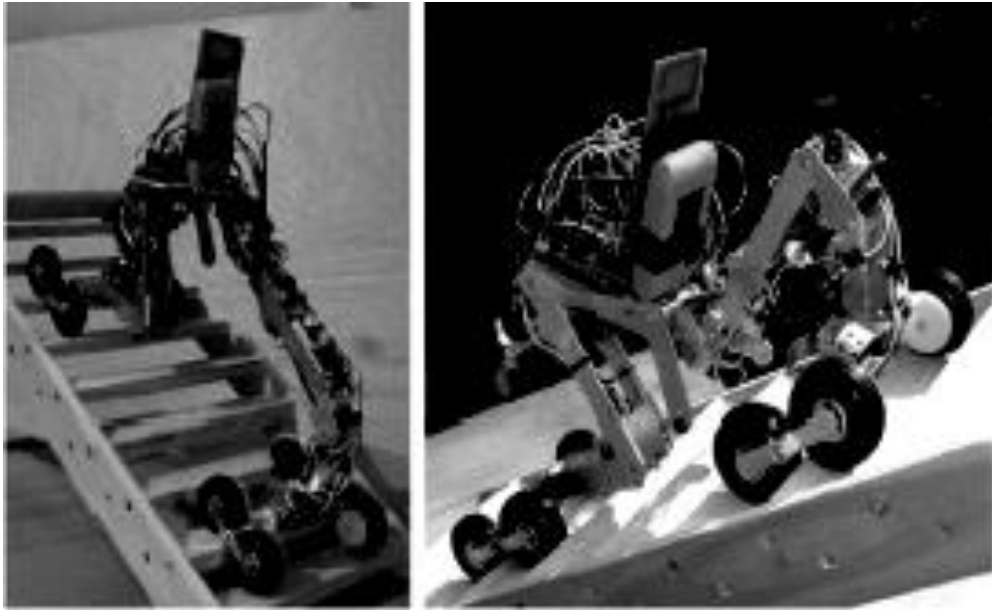




**Figure 2.3: customized climbing wheelchair**

the mechanical part was represented by combination of an innovative axles, highly stable metal body, bi-cycle sprocket with gear sets and screw joints to fix them all together, all lead by dc motors and chain transmission system [6].the electronic part consisted of multiple sensors such as ultrasonic sensor, accelerometer, joystick and peripheral modules such 16x2 LCD, driven by 5V supply from GR-KAEDE board [6].according to their simulation the robot provided The lowest point of stability during moments when the driving wheels leave the ground and the robot's driving wheels roll over the first and second steps.'' The main reason is that the driving wheels are suddenly suspended in the air. This has the result that the robot's rolling fulcrum moves forward substantially and thus it inclines to tumble backwards more easily'' [6] . The former result was proved in the tracked mobile robot's stairs climbing experiments [7].

The applications of Wheeled robots was greatly encountered in many designs due to simplicity, light weight, compact, have a smaller energy consumption with respect to track devices and the ease of manipulating wheels to construct different shapes therefore presenting continuous motion . One application of such a technique is inpatient rehabilitation, where stair climbing could greatly enhance mobility and thus quality of life, of people confined to wheelchairs. Lawn and Shiatsu [8] provided a design in this category shown in figure 2.4 using two (forward and rear) articulated wheel clusters attached to movable appendages.



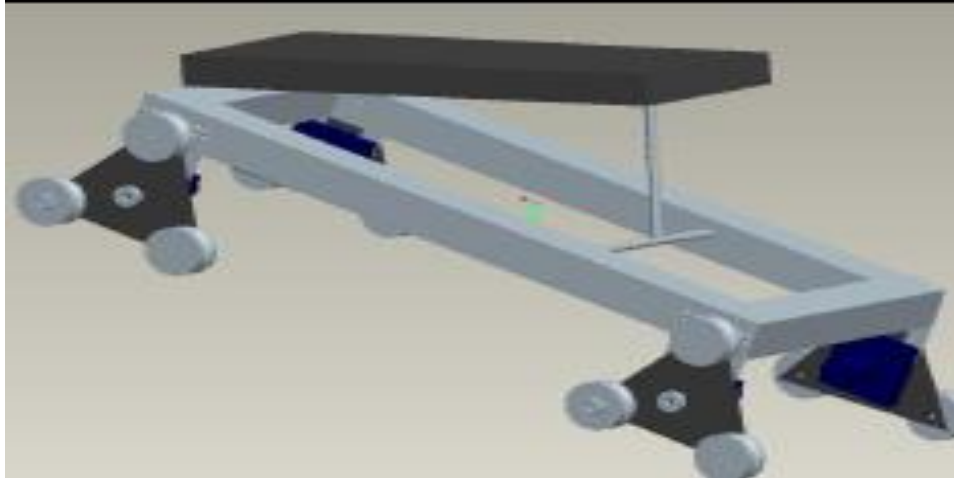
**Figure 2.4: Lawn and Shiatsu design**

The robot was equipped with step-contact sensors, but relies on user steering and is thus only semi-autonomous. A number of products existing on the commercial market such as, Magic Wheels and Max Sella Stair Lifter [9].magic wheels is a two geared manual wheel for step climbing, could maneuver over uneven terrain and it is not battery powered nevertheless it is expensive and user need a comprehensive and balanced upper body strength .max sella stair lifter is used to ascend normal set of stair but it does not promote user independence [9] . Pyra-Aid™, a design that was produced by J-Robert [9].Shown in figure 2.5 developed the common manual wheelchair frame adding a tri-wheel pat in between the clusters wheels. The design required low maintenance and can overcome curbs of different sizes, still, it requires progressive testing, alternative material and mass manufacturing processes investigation.



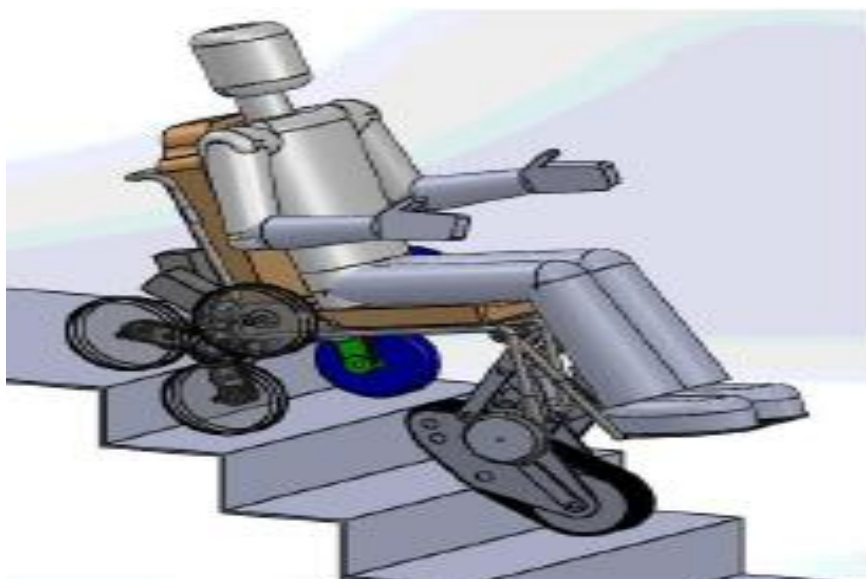
**Figure 2.5: Pyra-Aid™, a design**

Sandeep H.Deshmukh presented Stair Climbing Transporter (SCT) shown in figure 2.6 in which each wheel was formed in triangular shape with pulley in each head using belt system mechanism with control system [10].



**Figure 2.6: Sandeep H.Deshmukh Stair Climbing Transporters (SCT)**

the design showed a great performance in moving in terrines and stairs though it complied different limitation such us the fast wearing of the belts, technical failure of the control system and the unfit able constant speed which need to be variable [9] i.e. slow on climbing and fast on flat ground. G. Quaglia , W.Franco , and M. Nisi presented a another design in the form of track-wheel hybrid locomotion shown in figure 2.7 that uses wheels for moving on flat ground and tracks for stair climbing [11] .examples of similar idea had been reported by Morales R., Feliu V., González A. and Pintado P , Sugahara Y., Yonezawa N. and Kosuge K and Yuan J. and Hirose S [12] [13] [14].



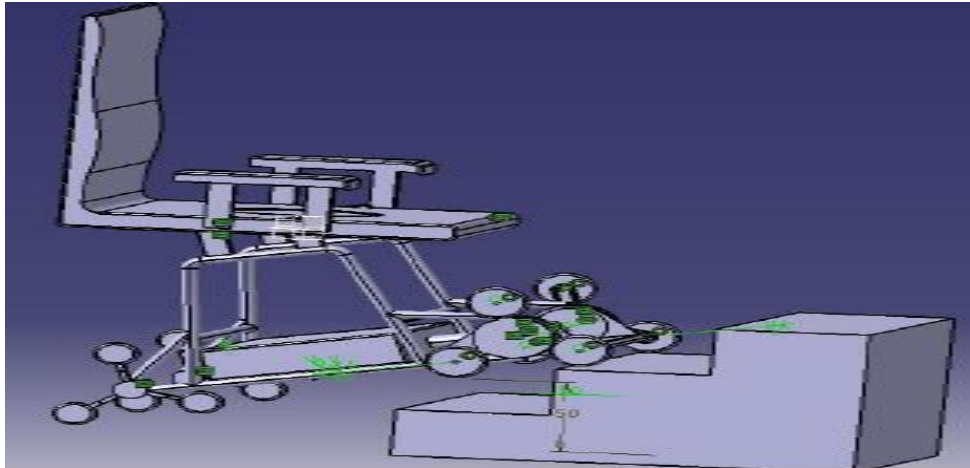
**Figure 2.7: track-wheel hybrid locomotion**

The design was a development of three versions of a stair climbing wheelchair concept called Wheelchair's .it is consisted of three functional elements; locomotion unit (tri-wheel), track and seat all connected in frame with a transmission element composed of the locomotion motors and their transmission systems. The design showed better performances with respect to other wheelchairs in terms of simplicity, cost reduction and autonomy. However the sensor system, the control logic and the complete mechatronic design were still under construction and need a further research and also, a dynamic analysis of wheelchair during different working conditions in order to evaluate if its behavior will be compatible with design requirements is not achieved [11]. R Rajasekar1, K P Pranavkarthik, R Prashanth, S Senthil Kumar and A Sivakumar provided a different design in the form of wheeled mobility, their design was objective by a wheel equally spaced with  $72^\circ$  shown in figure 2.8 it is manually operated and can travel in both flats and staircases.



**Figure 2.8: wheeled mobility design**

They've tried to minimize the cost of component as possible so as to be affordable for middle income class. In the other hand it lacked brake system which minimize the stability [15].Franco et al did work related to development of a stair climbing wheelchair that can move in structured and unstructured environments, climbing over obstacles and going up and down stairs [11].Tadakamalla Shanmukh Anirudh and Jyoti Pragyan Satpathy provided an ergonomically electric wheelchair with climbing stair functionality shown in figure 2.9 using also the mechanism of triwheel ,the design presented three part; the frame, the seat and the links their main problem was that the frame and wheels were designed and developed through the mathematical calculations from the statistical data of dimensions of staircases in Indian houses [16] taking out the universalism of the design .



**Figure 2.9: an ergonomically electric wheelchair with climbing stair functionality**

Another self propelled wheel chair for climbing stairs and slopes presented by A S Shriwaskar and S K Choudhary shown in figure 2.10. The design parts were tri-wheel Connecting rod, Crank, Frame and Supporting tri-wheel. Propulsion power was transmitted through motor and hand wheels.



**Figure 2.10: self propelled wheel chair for climbing stairs**

The front wheels are tri-wheels which take power form crank with the help of motor and are mainly used for climbing the stairs. Back tri-wheels were used to support the chair while climbing which reinforced the safety part of the design [17].

## **2.2 Component design**

### **2.2.1 Transmutation system design**

In this section the transmission system will be designed and the principle of the transmission mechanism will be considered first; then the gears inside of the planetary wheel system will be selected and assembled; the motors selection as well as the storage battery selection will determined later.

The main difference in most of the previous designs was the power transmission system either belt, chain or gear system. Table 2.1 present the main features that specify each type.




**Table 1.1: power transmission system**

<b>Belt drive</b>	<b>Chain drive</b>	<b>Gear system</b>
Rubber, light	metal, heavier	Small amount of friction.
often slip, work loss	strong	less chance of slipping
Fast wear	Low wear	transmitting high torque
Slight efficiency	Low efficiency	High efficiency
silent	Noisy	Quiet

### 2.2.2 Transmitting torque to and from shafts

In many machine designs, torque must be transmitted between shafts and gears, pulleys, chain-wheels and other hubs. In almost all cases, this must be done without allowing slip between the two parts [18]. As shown below table 2.2, there are a number of ways in which this torque transfer may be achieved.

**Table 1.2: ways for transmitting torque to and from shaft**

<b>Keys</b>	A keyway is machined into the shaft and a corresponding groove into the bore of the hub. The key fits simultaneously into both grooves, locking them together. The key is subjected to direct shear.	
<b>Grub screws and set screws</b>	These are regarded as light-duty attachments. Sometimes the end of the screw merely bears against the surface of the shaft. In other cases (dog-end or cone-end screws) the end of the screw may enter a drilled hole in the shaft	
<b>Splines</b>	Are essentially axial grooves or recesses which are machined into the shaft, very like a series of keyways. Splines are an integral part of the shaft (cf. keys, which are loose parts). Corresponding grooves are cut into the bore of the hub so that the shaft/hub assembly forms a series of interlocking projections.	

	The resulting connection is stronger than a keyed joint and is used in heavy-duty Applications.	
--	---	--

### 2.2.2.1 Keys

A key seat is a longitudinal groove cut into a shaft for the mounting of a key, permitting the transfer of torque from the shaft to a power-transmitting element, or vice versa. The key fits simultaneously into both grooves, locking them together. The key is subjected to direct shear [19].

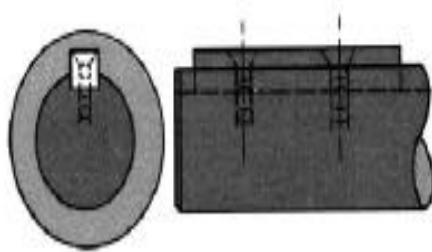


Figure 2.11: key seat

### 2.2.3 Shaft bearings



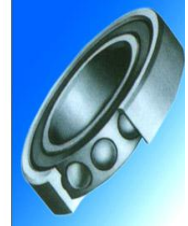

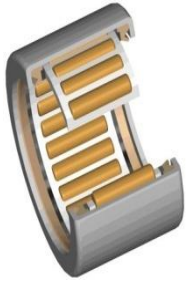

Bearings are one of the key components that determine the service interval for rotating machinery; they can even limit the life of the machine.

Bearings are used primarily to support rotating shafts in mechanical equipment. They can support heavy loads over a wide speed range and do it virtually friction free. In addition to Guide moving parts – wheel, shafts, pivots they keep the shaft moving smoothly and consistently while reducing friction. They are relatively inexpensive, and require little or no maintenance. Carry load in one or several directions while allowing frictionless motion in other directions [20].



#### 2.2.3.1 Types of rolling bearing

There are different type of bearing which differ in shape and functions shown on Table 2. 3 which provide types of rolling bearing, their description and advantages [21].

**Table 1-3 : types of rolling bearing**

<b>Types</b>	<b>discretion</b>		<b>advantages</b>	
Ball Bearing	Incorporates Hardened steel balls ,Steel balls Geometrically contact inner and outer race at a point This creates high stresses locally	Deep Groove Ball Bearings (radial)	<ul style="list-style-type: none"> <li>▪ Primarily for radial load carrying</li> <li>▪ Thrust load equal to 25% of radial load</li> <li>▪ Can get as large as 300K radial load capacity</li> </ul>	
		Double Deep Groove	<ul style="list-style-type: none"> <li>▪ Increases radial load</li> <li>▪ Less axial displacement</li> </ul>	
		Angular contact ball bearing	<ul style="list-style-type: none"> <li>▪ Increased thrust load due to increase in lateral contact area between ball and race</li> <li>▪ Axial rigidity</li> </ul>	
		Thrust Bearings	<ul style="list-style-type: none"> <li>▪ Used in applications with significant thrust load such as clutch release</li> </ul>	
Roller Bearings	Hardened steel cylindrical rollers Line contact deforms into areas larger than ball bearings	Needle Bearings	<ul style="list-style-type: none"> <li>▪ As the number of rollers goes up the greater the contact area</li> <li>▪ The greater the contact area the greater the load</li> </ul>	
		Spherical Roller Bearings	<ul style="list-style-type: none"> <li>▪ Centers inner race about shaft to avoid binding</li> </ul>	



	Capable of carrying higher radial loads	Tapered Roller Bearing	<ul style="list-style-type: none"> <li>▪ Support high thrust loads (wheel bearing)</li> <li>▪ Supports radial load (car weight) while supporting thrust loads (cornering)</li> <li>▪ Wheel rotates with little resistance/friction</li> </ul>	
		Thrust Roller Bearings	<ul style="list-style-type: none"> <li>▪ Used in applications with significant thrust load</li> </ul>	

### 2.2.3.2 The Bearing Selection Process

In order to select the most appropriate bearing for an application, it is very important to understand the expected operating conditions of the bearing. The main bearing selection criteria will be covered in this section.

#### 1. Mounting Space

When an application is designed, a primary consideration is for the shaft to have the proper strength and rigidity. Consequently, the minimum required shaft diameter is determined followed by a determination of the allowable housing size, weight, and material needs based on the application environment and loads.

#### 2. Loading

Load type, magnitude, and direction of loads are all key in determining the proper bearing for a particular application. The load types are normally described as

1. When the direction of the load (weight being moved) is at right angles to the shaft, it is called a “radial” load. The load pushes down on the bearing (fig. 1).
2. When the direction of the load is parallel to the shaft, it is called a “thrust” load. The load pushes sideways on the bearing (fig. 2).
3. When the direction of the load is a combination of radial and thrust, the load pushes down sideways on the bearing. This combination is called an “angular” load (fig.3)

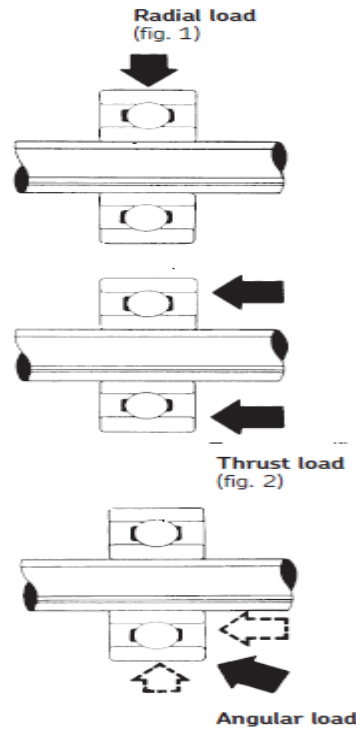


Figure 1.12: load type

### 3. Speed Requirements

Speed requirements are normally expressed in RPM's (Revolutions per Minute). Normally the first question regarding operating speed is what the expected maximum RPM's is.

### 4. Rigidity Requirements

In applications such as machine tool spindles and automobile final drives, bearing rigidity can be a determining factor of its desirability. Rigidity can be defined as the resistance of a bearing to elastic deformation at the point where the rolling elements contact the raceway surface. The higher the bearing rigidity the better the resistance to load induced deformation . Elastic deformation is less of a problem with line contact roller bearings than point contact ball bearings.

#### 2.2.3.3 Bearing life

When bearings are rotated under load and subjected to repeated contact stresses, wear will eventually result in the raceway material flaking off. The effective life of a bearing is usually defined in terms the total number of revolutions and until flaking occurs it is described as the bearing service or fatigue life. Bearing service (fatigue) life varies depending on design, size, materials, manufacturing methods, and operating conditions [21].

For bearings operating at fixed constant speeds, the basic rating life (90% reliability) is expressed in the total number of hours of operation. The basic dynamic load rating is an

expression of the load capacity of a bearing based on a constant load which the bearing can sustain for one million revolutions (the basic life rating). For radial bearings this rating applies to pure radial loads [21] .

# Chapter Three

## Theoretical Background

### 3.1 Concept Development

In this section we described the main idea of the design, it's operation mechanism include it's movement on stairs and flat surfaces mechanism.

#### 3.1.1 Design Concept

The idea behind our design was to design a mechanism to help disabled person move upstairs easily. The study focused on the tri-star wheel robot design. The focuses are more on the gearing drive system and the tri-star wheel design which three wheels are arranged in an upright triangle with two on the ground and one above them, as shown in Figure 3.1. If either of the wheels in contact with the ground receives resistant, the whole system rotates over the obstruction. At rest, each Tri-Star wheel is likely to have two wheels in contact with the ground [20].

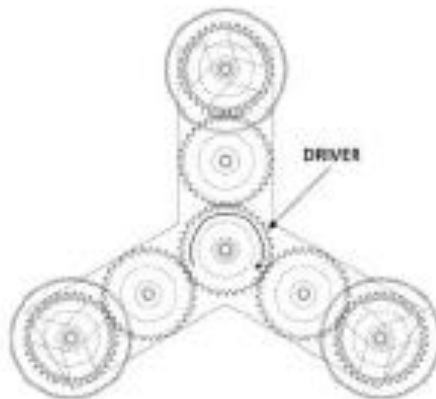


Figure 3.1: tri-star wheel structure

#### 3.1.2 Procedure of movement

Propulsion power for both conventional level operation and stair climbing operation is transmitted through the motor .Operation on level ground is similar to the operation of a conventional wheel chair.

### 3.1.3 Process for Climbing Stairs

Firstly the tri-star wheel comes in contact with the stairs then due to obstacle the whole front tri-star frame will rotate toward the obstacle. As the frame rotates the upper wheel rest on the next step and moves forward refer to Figure 3.2 .As the rear part is moving forward, it will push the front part to move along the vertical surface of the stair and finally climb onto the up surface of the stair. the front part is climbing to next step while the rear part is starting contact with the stair. In this situation, the rear part vertically moves along the stair under the pulling forces of the front part. In addition, the rear part motor is also actuated to easily climb the rear part. In this way, the robot will perform the process of climbing stair.

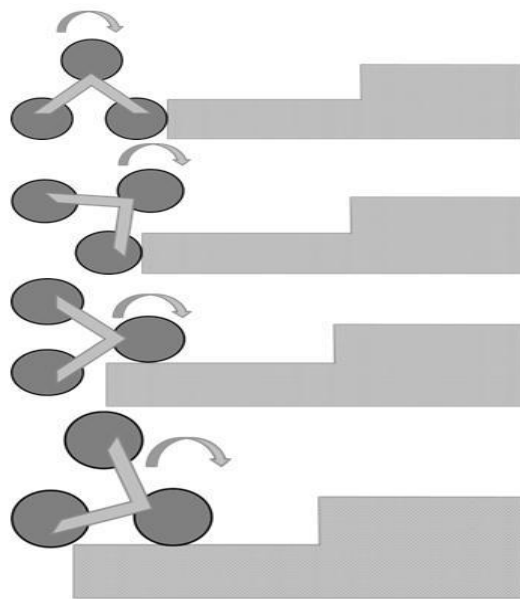


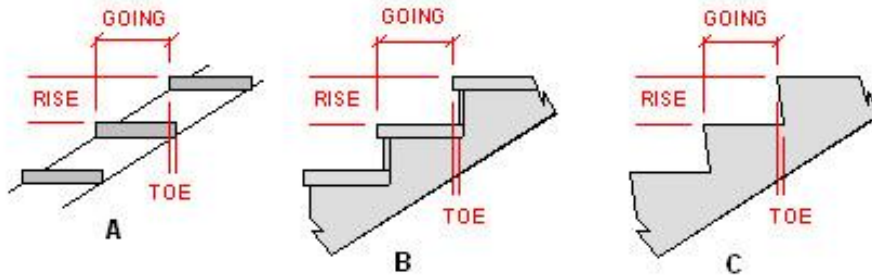
Figure 3.2: Process for Climbing Stairs [21]

## 3.2 Determination Of The Basic Parameters

The range of the structure size of the tri-star wheels system is determined by the staircase, and the wheels of the wheelchair needs a stable support on the stairs during the process of climbing stairs, if the diameter of the wheels are too large, the wheelchair is unable to support itself on the stairs, and it is also not good for reducing the volume of the wheelchair; if the diameter is too small, the wheelchair will have a low efficiency when it moves on the flat ground, and it has a poor ability to adapt to the terrain. Depending in staircase we can determine the dimensions of the holder that carry the wheel which determines whether the robot is able to climb the stairs. The step-wide  $G$  and the step-height  $R$  are determined by the stair design rules, which are shown in the table 3.1 [22].

**Table 0.1: Different type of stairs**

STEP-HEIGHT(R)		STEP-WIDE (G)		SLOPE RELATIONSHIP $=2R+G$	
MAXIMUM	MINIMUM	MAXIMUM	MINIMUM	MAXIMUM	MINIMUM
190	115	355	240	700	550



**Figure 3.3: Different type of stairs [22]**

Apparently, the width of the staircases should not be less than 240mm and the height should not be more than 190mm. So here the width of the stairs  $b=300\text{mm}$ , and the height  $h=170\text{mm}$  are chosen, as the calculation reference of our design.

From all of the above we found that in the design of Tri-Star wheel, five parameters are important which are the height of the stairs (a), width of stairs (b), radius of regular wheel (r), radius of Tri-Star wheel, the distance between the center of Tri-Star wheel and the center of its wheel (R) and the thickness of holders that fix the wheel on its place on Tri-Star wheel (t).

### 3.2.1 Tri-Star Wheel holder

Three wheels are arranged in a triangular array, such that centers of each of the wheels coincide with vertices of an equilateral triangle. Now the side of an equilateral triangle (R) and radius of the wheel (r) are calculated using certain equations, which are described below in figure 3.4 [20].

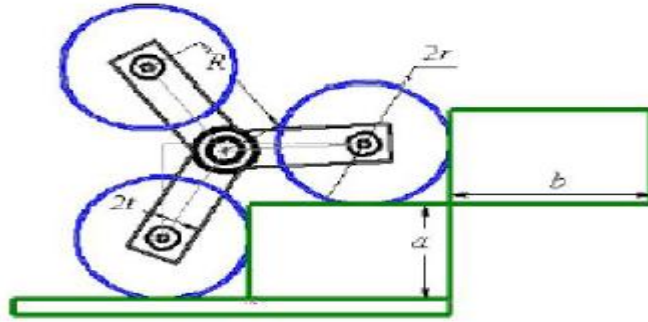


Figure 3.4: an equilateral triangle (R) and radius of the wheel (r)

$$R = \sqrt{\frac{(a^2+b^2)}{3}} \quad (1)$$

Where,

R = the distance between the center of Tri-Star wheel and the center of its wheel

a = the height of the stairs

b =width of stairs

r = radius of regular wheel

The maximum value of the thickness of holder ( $t_{\max}$ ) to avoid the collision between the holder and stairs

$$t_{\max} = \frac{ar(3-\sqrt{3})+br(3+\sqrt{3})+a(\sqrt{3}a-\sqrt{3}b)}{6R} \quad (2)$$

Where,

t = the thickness of holders that fix the wheel on its place on Tri-Star wheel

r = radius of regular wheel

### 3.2.2 Radius of regular Wheel

Minimum radius of regular wheel ( $r_{\min}$ ) to prevent the collision of the holders to the stairs is derived as follows (refer to Figure 3.5a) [20]

$$r_{\min} = \frac{6Rt + a(3b - \sqrt{3}a)}{(3 - \sqrt{3})a + (3 + \sqrt{3})b} \quad (3)$$

Maximum radius of regular wheel ( $r_{\max}$ ) to prevent the collision of the wheels together (refer to Figure 3.5b) [20].

$$R_{\max} = \frac{\sqrt{(a^2 + b^2)}}{2} \quad (4)$$

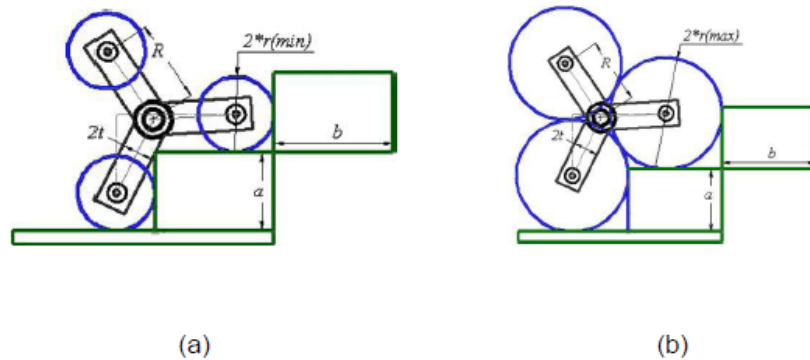


Figure 3.5: (a) Minimum radius of regular wheel, (b) Maximum radius of regular wheel

### 3.2.3 Dimension of key seat

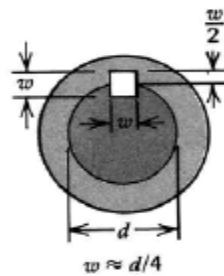


Figure 3.6 : key seat dimensions

The width of key seat dimension calculated by the equation below [19] .

$$W = \frac{D}{4} \quad (5)$$

## 3.3 Transmission system

### 3.3.1 Working principle for the transmission system

The work principle when input comes from motor driver to the central (solar) gears of the planetary wheels system, central gear transfer input to the follower gear through idler gear (refer to figure 3.7) because we want all follower gears to rotate at the same direction of driver as shown below [24] .



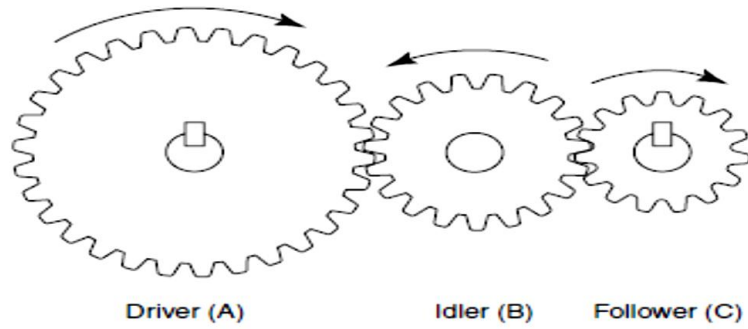


Figure 3.7: Working principle for the transmission system

And this transmission occur according to movement ratio between gears

$$\text{movement ratio} = \frac{\text{speed of driver}}{\text{speed of follower}} = \frac{\text{teeth of follower}}{\text{teeth of driver}} \quad (6)$$

That the arc length of the distance traveled by one gear must equal that of the other that is, the distance traveled along the surface of each gear is the same.

### 3.3.2 Gear Selection

The specifications of gears are obtained According to the center to center distance at holder (R) the pitch diameter of gear have chosen to be 100 mm refer to figure 3.8, all planetary gears have same dimension that we need to transmission same power to all wheels [27] .

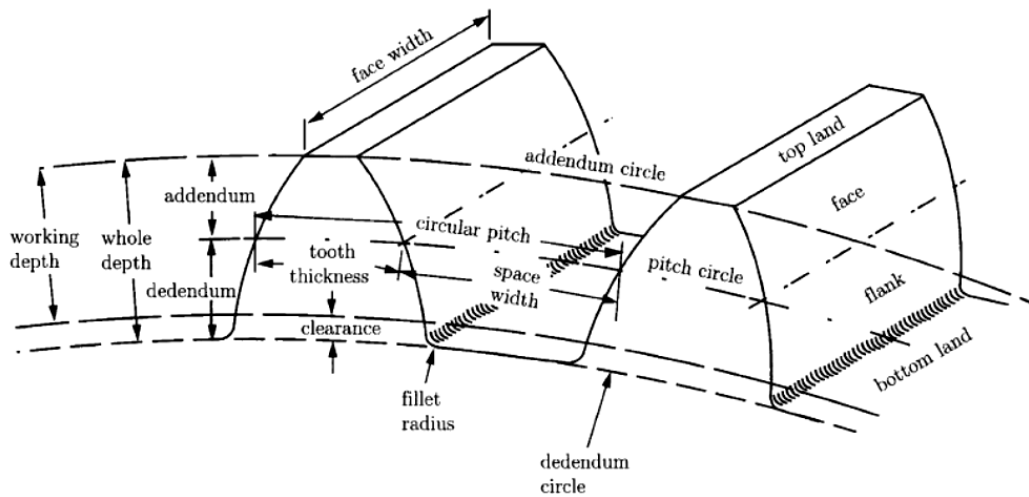


Figure 3.8: Gear specifications

#### 1. Module

It is the ratio of the pitch circle diameter in millimeters to the number of teeth. It is usually denoted by ( $m$ ) according to the size requirements of the triangle star wheel and in order to decrease the installation accuracy.

## 2. Pitch diameter (D)

It is the diameter of the pitch circle (an imaginary circle which by pure rolling action would give the same motion as the actual gear).

$$D = T \times m \quad (7)$$

Where,

D = Pitch diameter

T = Number of teeth

m = Module

Then

$$T = \frac{D}{m} \quad (8)$$

## 3. Pressure angle or angle of obliquity

It is the angle between the common normal to two gear teeth at the point of contact and the common tangent at the pitch point. It is usually denoted by  $\phi$ . The standard pressure angles are  $14^\circ$  and  $20^\circ$ .

## 4. The outside diameter ( $D_o$ )

$$D_o = m(T + 2) \quad (9)$$

Where,

$D_o$  = The outside diameter

## 5. Total depth ( $h_t$ )

It is the radial distance between the addendum and the dedendum circles of a gear.

$$h_t = 2.25 \times m \quad (10)$$

Where,

$h_t$  = Total depth

## 6. Tooth thickness

It is the width of the tooth measured along the pitch circle.

$$\text{tooth thickness} = 1.57 \times m \quad (11)$$

### 3.4 Bearing calculations

The aim of bearing calculations is to estimate how long a bearing will last within a specified probability. In the theoretical calculation, failure is defined as the first sign of pitting, not when the whole bearing breaks down. Loads applied to the bearing generally include the weight of the rotating element itself, the load produced by the working of the machine, and the load resulting from transmission of power by the belt and gearwheel [21] .

#### 3.4.1 Load applied to the bearing by power transmission

The force working on the shaft when power is transmitted by belts, chains or gearwheels is obtained, in general, by the following formula [21]

$$K_t = \frac{T}{r} \quad (12)$$

Where,

$K_t$  = Transmission force

$T$  =: Torque, Nm,

$r$  =effective radius of gearwheel, m, inch

#### 3.4.2 Gear transmission

In the case of gear transmissions, the theoretical gear load can be calculated from the transmission force and the type of gear. With spur gears, only a radial load is involved. The simplest case is that of spur gears. In this instance, the tangential force  $K_t$  is obtained from the equation 3-12 and the radial force  $K_s$  can be obtained from the following equation [21].

$$K_s = K_t \cdot \tan \alpha \quad (13)$$

Where,

$K_s$  = radial force

$K_t$  = Transmission force

$\alpha$  = is the pressure angle of the gear.

Accordingly, the theoretical composite force,  $K_r$ , working on the gear is obtained from the following formula:

$$K_r = \sqrt{K_t^2 + K_s^2} \quad (14)$$

Where,

$K_r$  = the theoretical composite force

### 3.5 Motor Selection

To select a proper motor to drive this system we have to determine the following specification.

#### 3.5.1 Speed determination

Design standards of wheelchair state that the moving speed should not exceed  $v_{max} = 1.8$  m/s, [24]

$$N = \frac{v \times 60}{\pi \times d} \quad (15)$$

Where,

$N$  = angular speed of motor

$v$  = linear speed of robot

$d$  = diameter of gear

So the angular velocity of central gear is:

$$i = \frac{Z_2}{Z_1} = \frac{n_1}{n_2} \quad (16)$$

$i$  = the angular velocity of central gear

$Z_1$  = number of teeth

$Z_2$  = number of teeth

$n_1$  = the gear speed

$n_2$  = the gear speed

#### 3.5.2 Torque determination

$$T = \frac{P \times 60}{2 \times \pi \times N} \quad (1)$$

Where,

$T$ = Torque determination

$P$ = the power

### 3.5.3 Power checked

The rolling friction coefficient between tire and normal road surface is 0.02, which is decided by checking the mechanical design manual [28], and we take safety factor  $K_s=1.5$ , the power required when the wheelchair works is,

$$P = K_s \times Fmgv \quad (2)$$

Where,

$K_s$  =safety factor

$F$ = force

$m$ = mass

$g$ = gravity

$v$ = velocity

# Chapter Four

## Design

### 4.1 Introduction

The chapter describe the design of stair climber component's dimension, also it provide the details about applied materials, the improvement of the initial design and the forces analysis.

### 4.2 Methodology

The methodology followed in the thesis had been described from the collection of design specification required for design implementation till the process led to the final design using mechanical principles and SOLIDWORK 2016 software in the flow chart below

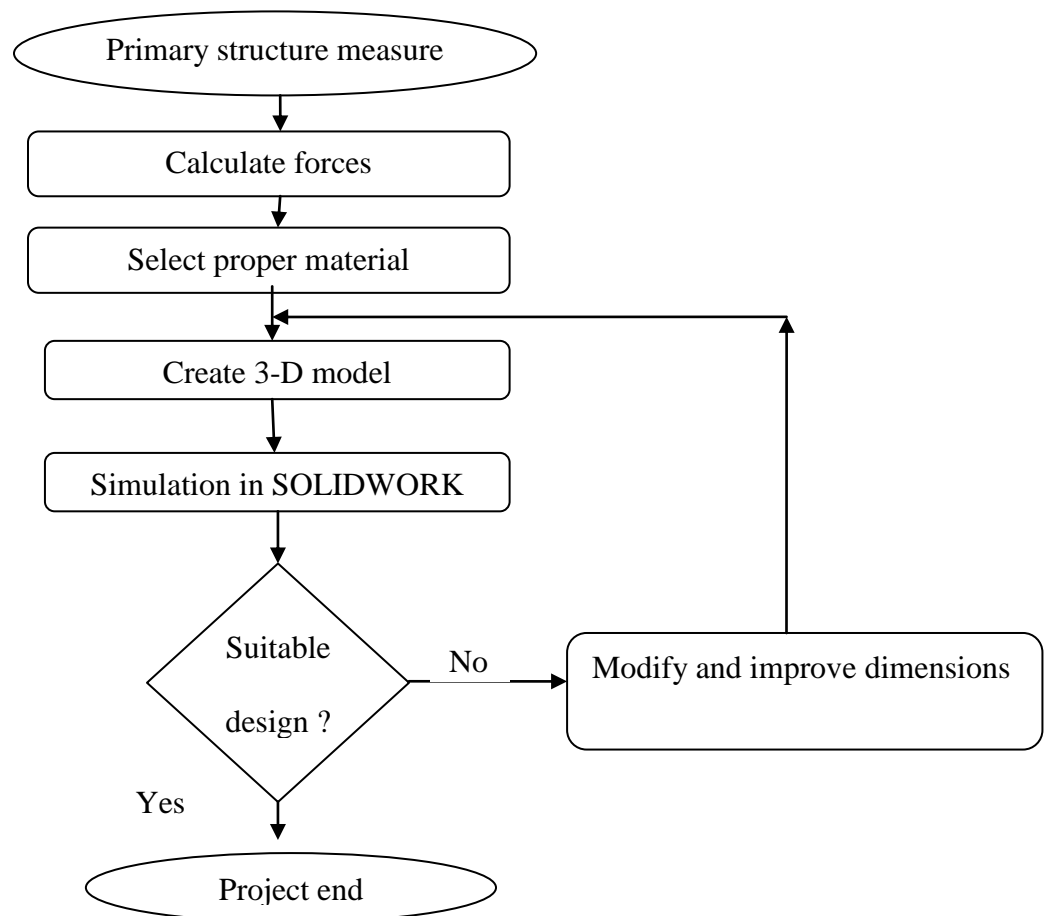


Figure 4.1: flow chart describing systematic procedures for methodology

### 4.3 Initial design Structure calculation

According to the project requirements, Star-wheel have been designed for traversing stair with 17 cm in height and 30 cm in width (a=17cm , b=30 cm).

#### 4.3.1 Determine baseline model dimension

We applied the dimension of stair on the equations shown in chapter 3 to obtain the acceptable dimension of our model

##### 4.3.1.1 Tri-Star Wheel holder

By using equation 3-1 we can get the radius of the holder with 17 cm in height and 30 cm in width (a=17cm , b=30 cm).

$$R = \sqrt{\frac{(17^2 + 30^2)}{3}}$$

$$R = 20cm$$

The maximum value of the thickness of holder ( $t_{max}$ ) to avoid the collision between the holder and stairs is derived by assume  $r=12$  cm refer to equation 3-2.

$$t_{max} = \frac{17 * 12(3 - \sqrt{3}) + 30 * 12(3 + \sqrt{3}) + 17 * (\sqrt{3} * 17 - \sqrt{3} * 30)}{6 * 20}$$

$$= 13.2 cm$$

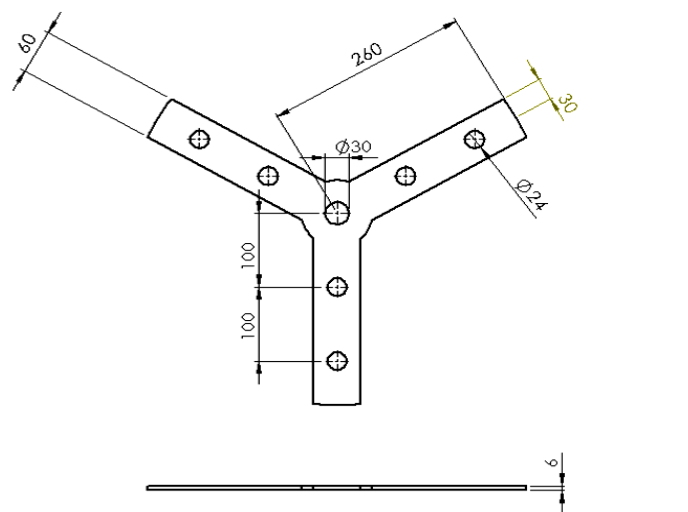


Figure 4.2: The dimension of holder at solid work

### 4.3.1.2 Radius of regular Wheel

Minimum radius of regular wheel ( $r_{\min}$ ) refer to equation 3.

$$R_{\min} = \frac{6 * 20 * 3 + 17(3 * 30 - \sqrt{3} * 17)}{(3 - \sqrt{3}) * 17 + (3 + \sqrt{3}) * 30}$$

$$r_{\min} = 8.5 \text{ cm}$$

Maximum radius of regular wheel ( $r_{\max}$ ) refer to equation 4.

$$R_{\max} = \frac{\sqrt{(17^2 + 30^2)}}{2}$$

$$r_{\max} = 17.2 \text{ cm}$$

Then the regular wheel diameter range from (17 cm to 34.4cm) and the selected wheel is 24cm diameter as shown at figure 4.3

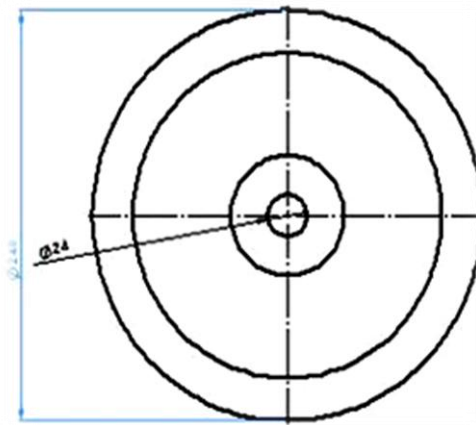


Figure 4.3: the wheel

### 4.3.2 Gear Selection

The gears inside of the planetary wheels is shown in figure 4.4, and now the teeth and modulus for each gear will be selected using equations from (7-11) as shown on table 4.1 .



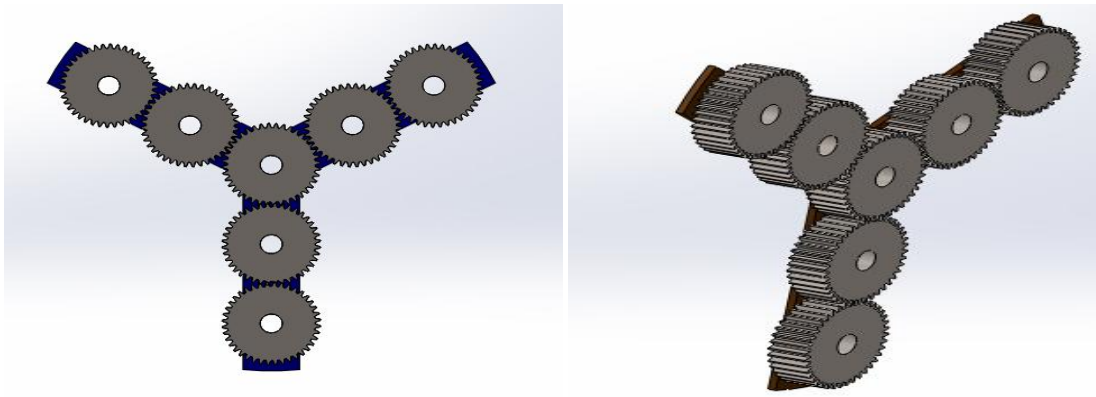


Figure 4.4: The gears inside of the planetary wheels

NUMBER OF TEETH

$$T = \frac{100}{2.5}$$

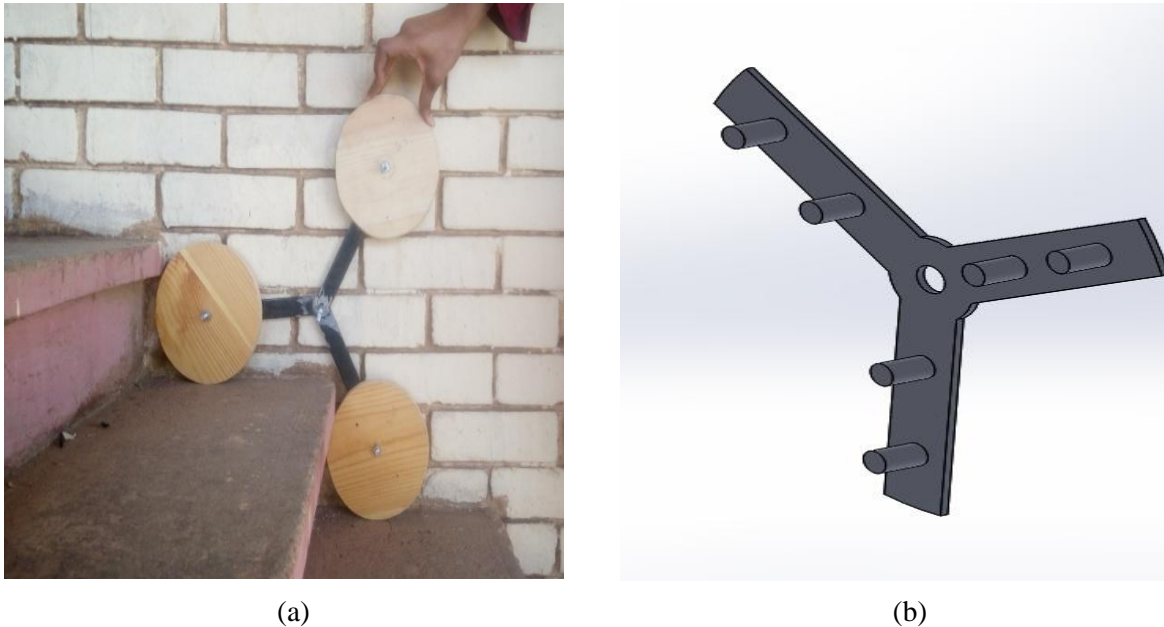
=40 teeth

Table 0.1: gear specification

Specification	value
Pitch diameter (Equation 7)	100m
Outer diameter (Equation 9)	105m
Hole diameter	15 mm
Module	2.5
whole depth (Equation 10)	5.6mm
Width	30mm
Pressure angle	20°
Tooth thickness (Equation 11)	4mm

### 4.3.3 Simulation Study

Manual Simulation study was provided in order to verify the reliability of the design. Manual simulation is a pure climbing task with the prototype tri-star wheel being placed on the stairs manually by an operator, as shown in Figure 4.4. The tasks were repeated ten times without any serious problem.



**Figure 4.5: (a) manual simulation, (b) software simulation**

Software simulation is provided by Solid Work 2016. The main objective is to simulate the movement of tri-star wheel assembly and the connection shaft between the body sections. The study started with the development of 3D design of the robot, as shown in Figure 4.4(b). The design of the stair was developed in simulation environment, and the simulation study is provided. From simulation the motion of wheel didn't follow the motion of gears and holder didn't respond to power transmitted from motor so we didn't achieve our main objective so that we have to improve the design.

## 4.4 Improved design

This section provides to improve the initial design to assure that we get proper transmission of power to wheel through gears at the same speed and direction. to achieve this improvement, the dimension of the shaft that carry gears and wheels should be changed to suit wheel and gear ,in addition to locate bearing that prevent holder from rotate according to the rotation of the shaft .

### 4.4.1 Holder

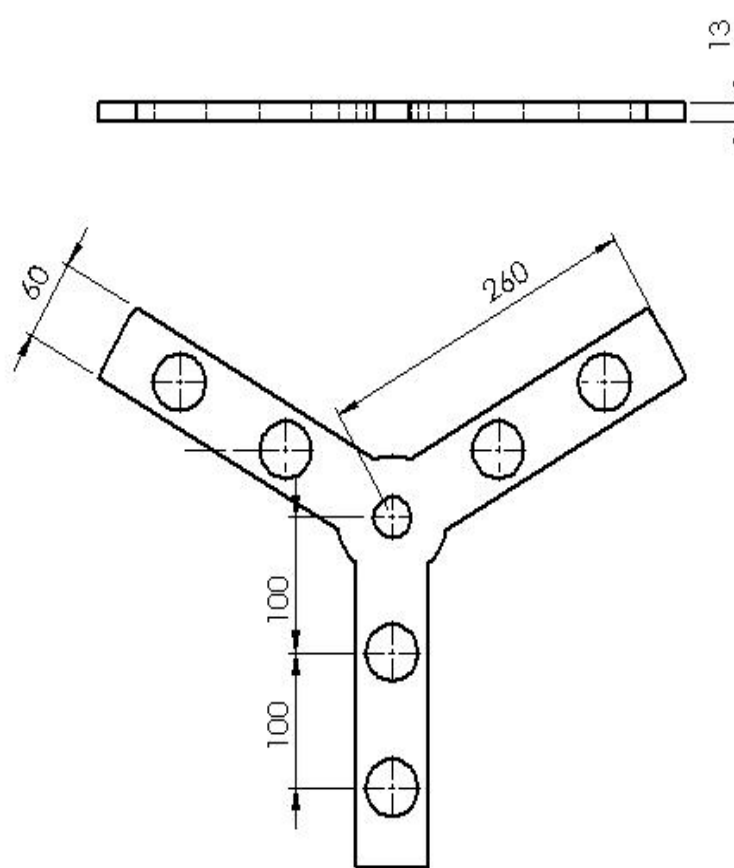


Figure 4.6: The holder

### 4.4.2 Shaft

Shafts have numerous changes in diameter to accommodate bearings and gears as well as features such as keyways to provide torque transmission.

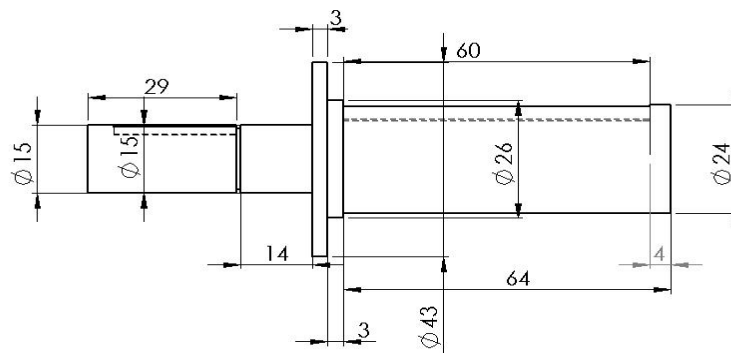


Figure 4.7: Shaft with The location of support bearing is shown schematically. There are two key seat for fixing gear (on lift-side) and wheel (on the right-side) with the shaft.

### 4.4.3 Key seat

The width of the key calculate by Equation 3-5

$$w = \frac{D}{4}$$

*for gear*

$$w = \frac{15}{4} = 3.75$$

*for wheel*

$$w = \frac{24}{4} = 6$$

The part of key attached with gear and wheel calculated by following equation for gear

$$\frac{1.75}{2} = 1.875$$

For wheel

$$\frac{6}{2} = 3$$

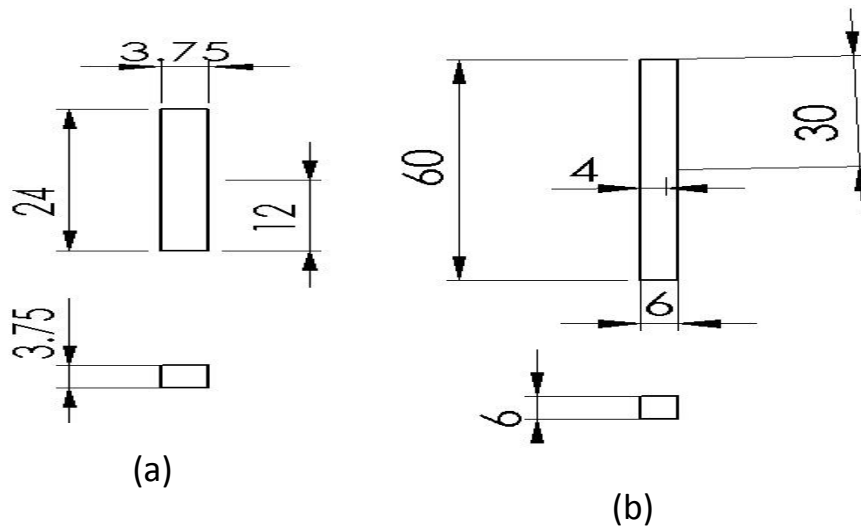


Figure 4.8 a) gear key, b) wheel key

### 4.4.4 Wheels

We changed the hole's shape and dimension to be suitable for key dimensions but the dimension of the outer diameter is still similar to initial design wheel diameter

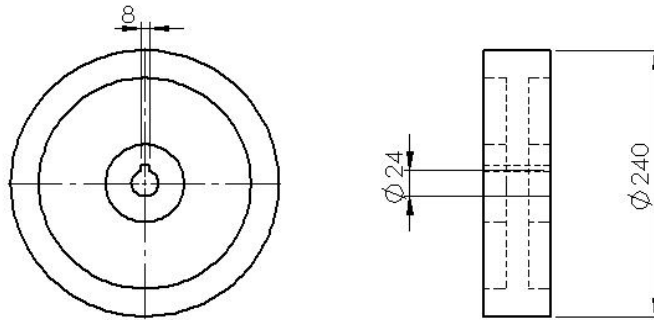


Figure 4.9: the wheel dimension

#### 4.4.5 Gears

We have two types of gear here which have the same dimensions but differ in the inner diameter: Wheel gear that transmit power to wheel and gear that transmit power from motor to the middle gear ( refer figure 4.7) and One for the power transmission from the middle gear to the wheel gear (refer figure 4.8).

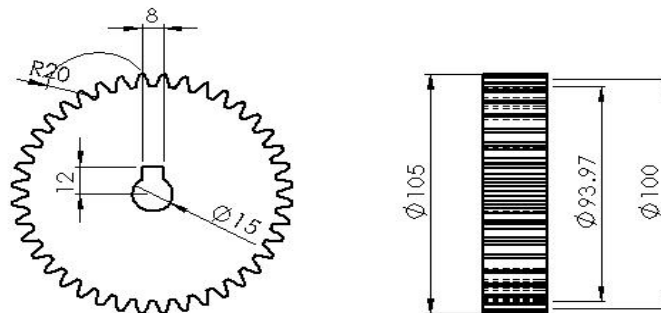


Figure 4.10: gear with key seat

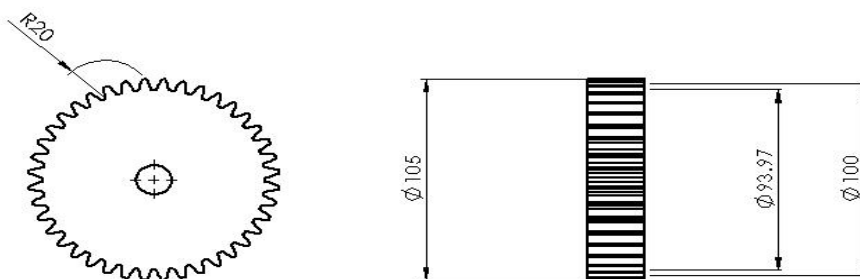


Figure 4.11: middle gear

#### 4.4.6 Force estimation

Total Weight of Whole System = 4 (Weight of Star Wheel) + Weight of Drive Gear Motor +  
Weight of battery

$$\text{Total weight of whole system} = 4 \times 4 + 5 + 9 = 30\text{Kg}$$

$$\text{Chair weight} = 29.6 \text{ kg}$$

$$\text{Person weight} = 80 \text{ kg}$$

For rolling applications, generally preferred value the coefficient of friction is 0.2.

Total pulling Weight = Total weight of whole system + chair weight + person weight

Hence,

$$\text{Total pulling weight} = 29.6 + 30 + 80$$

$$\text{Total pulling weight} = 139.6 \text{ kg}$$

Maximum Pull = Total pulling weight  $\times$  Coefficient of friction

$$= 139.6 \times 1.2 = 167.52 \text{ Kg}$$

Where, consider  $g = 9.8 \text{ m/s}^2$

$$\text{Maximum pull force} = 167.52 \times 9.8$$

$$= 1,641.7 \text{ N}$$

For one side pull force = 410.4 N

#### 4.4.7 Bearing selection

The Load applied to the bearing by power transmission calculated by equation 12 that shown early in (chapter 3)

$$K_t = \frac{61.56}{0.52}$$

$$K_t = 118.38 \text{ N}$$

. With spur gears, only a radial load is involved. The radial force  $K_s$  can be obtained from equation (13)

$$K_s = K_t \cdot \tan \alpha$$

$$K_s = 118.38 \times \tan 20$$

$$K_s = 264.84 \text{ N}$$

Composite force,  $K_r$ , working on the gear is obtained from the following formula:

$$K_r = \sqrt{K_t^2 + K_s^2}$$

$$K_r = \sqrt{(118.38)^2 + (264.84)^2}$$

$$K_r = 290.095 \text{ N}$$

$$\text{actual load} = K_r \times f_z$$

$$\text{actual load} = 290.095 \times 1.05$$

$$= 304.6 \text{ N}$$

The selected bearing should withstand the resultant Composite force

## 4.5 Motor selection

To select the proper motor the specification required had been determined as followed.

### 4.5.1 Speed determination

The driving mechanism is powered by 4 DC motor that coupled to the far side of the wheel .the robot is designed to have a maximum velocity of 50cm/s= 1.8km/hr .considering the total force of each wagon (410.4 N)

Required RPM (N)

$$N = \frac{v \times 60}{\pi \times d} \quad (16)$$

$$= \frac{50 \times 60}{\pi \times 0.1}$$

$$= 95.49 \text{ rpm}$$

So the angular velocity of central gear is:

$$i = \frac{Z_2}{Z_1} = \frac{n_1}{n_2} \quad (17)$$

$$n_1 = n_2 = 95.49 \text{ rpm}$$

## 4.5.2 Torque determination

$$T = \frac{410.4 \times 60}{2 \times \pi \times 95.49} \quad (18)$$

$$T = 41.04 \text{ N.m}$$

Consider the service factor is 1.5

Final output Torque ( $T$ ) = required torque  $\times$  Service factor

$$= 410.4 \times 1.5$$

$$= 61.56 \text{ N.m}$$

Final output RPM ( $n$ ) = 95.49 rpm

## 4.5.3 Powered checked

Get safety factor  $K_s=1.5$ , the total weight of a person and the wheelchair is 148.8 kg. And the power required when the wheelchair works is,

$$P = 1.5 \times 0.02 \times 167.56 \times 9.8 \times 0.5 \quad (19)$$

$$= 24.63 \text{ W}$$

For 4 motors we need total power

$$P_T = P \times 4$$

$$= 98.7 \text{ W}$$

The motor is primarily used as the engine when the wheelchair moving on the ground or climbing up and down stairs, so the rated power should be much bigger than 100W.

## 4.6 Shaft analysis

In a given shaft, several different stress conditions can exist at the same time. For any part of the shaft that transmits power, there will be a torsion shear stress, while bending stress is usually present on the same parts the bending stresses will be assumed to be completely reversed and repeated because of the rotation of the shaft (see appendix A).



#### 4.6.1 Normal stress

$$\text{area} = 2\pi r^2 + h(2\pi r) \quad (21)$$

$$\text{area}_a = 2\pi \times 12^2 + 66(2\pi \times 12) = 5881\text{mm}^2$$

$$\text{area}_b = (2\pi \times 21^2) + 37(2\pi \times 21) = 7652.9\text{mm}^2$$

Groove rings

$$\text{area}_c = (2\pi \times 27.52) + 3(2\pi \times 27.5) = 3309.6\text{mm}^2$$

$$\text{area}_d = (2\pi \times 7.52) + 3(2\pi \times 7.5) = 1484.4\text{mm}^2$$

$A \equiv \text{gear shaft part}$

$B \equiv \text{wheel shaft part}$

$$\sigma = \frac{F}{A} \quad (20)$$

$$\sigma_a = \frac{68.4}{5881} = 0.0116\text{ N/mm}^2$$

$$\sigma_b = \frac{68.4}{7652.9} = 0.0089\text{ N/mm}^2$$

For groove rings:

$$\sigma_c = \frac{68.4}{3309.6} = 0.206\text{ N/mm}^2$$

$$\sigma_d = \frac{68.4}{1484.4} = 0.046\text{ N/mm}^2$$

#### 4.6.2 Torsion shear stress

Torque of shaft = 61.56 N.m

$$\sigma_s = \frac{T.D}{j} \quad (22)$$

$$j = \frac{\pi D^4}{32} = T.D \times \frac{32}{\pi D^4} \quad (23)$$

By applying equation (24) in appendix A

$$a_1 = \frac{\pi D^3}{32} = \frac{\pi \times 24^3}{32} = 1357.1$$

$$a_2 = \frac{\pi \times 15^3}{32} = 331.33$$

$$\sigma_{s1} = \frac{61.56}{1357.1} = 0.0453 \text{ N/mm}^2$$

$$\sigma_{s2} = \frac{61.56}{331.33} = 0.1857 \text{ N/mm}^2$$

### 4.6.3 Load at the gear pitch circle

Using equation 25 to obtained load as following

$$F_t = \frac{2T}{D_p} = \frac{2 \times 61.56}{0.1} = 1231.2 \text{ N}$$

Resultant force on the shaft

$$F_r = \frac{F_t}{\cos \theta} = \frac{1231.2}{\cos 20} = 1323.8 \text{ N}$$

### 4.6.4 Shear stress

$$\tau = \frac{16 T}{\pi D^3} \quad (27)$$

$$\tau_1 = \frac{16 \times 61.65}{\pi \times 24^3} = 0.022 \text{ N/mm}^2$$

$$\tau_2 = \frac{16 \times 61.65}{\pi \times 15^3} = 0.0928 \text{ N/mm}^2$$

In groove ring:

$$\tau_1 = \frac{16 \times 61.56}{\pi \times 42^3} = 0.00423 \text{ N/mm}^2$$

$$\tau_2 = \frac{16 \times 61.56}{\pi \times 43^3} = 0.0039 \text{ N/mm}^2$$

### 4.6.5 Bending stresses

$$\sigma_x = \frac{M Y}{I} \quad (28)$$

$$I = \frac{\pi \times D^4}{64} \quad (29)$$

$$I_1 = \frac{\pi \times 24^4}{64}$$

$$= 28.27 \text{ mm}^2$$

$$I_1 = \frac{\pi \times 15^4}{64}$$

$$= 11.04 \text{ mm}^2$$

For groove ring

$$I_1 = \frac{\pi \times 42^4}{64}$$

$$= 86.59 \text{ mm}^2$$

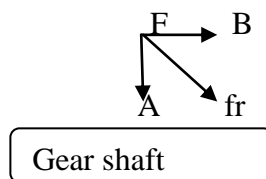
$$I_1 = \frac{\pi \times 43^4}{64}$$

$$= 90.76 \text{ mm}^2$$

$$M = ?$$

$$f_r = 1323.8 \text{ N}$$

$$\theta = 20^\circ$$



$$F = f_r \times \cos\theta \quad (30)$$

$$A = 1323.8 \times 0.939$$

$$= 1243 \text{ N}$$

$$B = 1323.8 \times 0.342$$

$$= 452.73 \text{ N}$$

Considering force is distributed equally along the shaft for balancing the system:

$$f = \frac{68.4}{2}$$

$$= 34.2 \text{ N}$$

But the two parts of the shaft are not equal in length; therefore it has been taken in ratio where its lengths are in the ratio of

$$66:37$$

Divide by 66

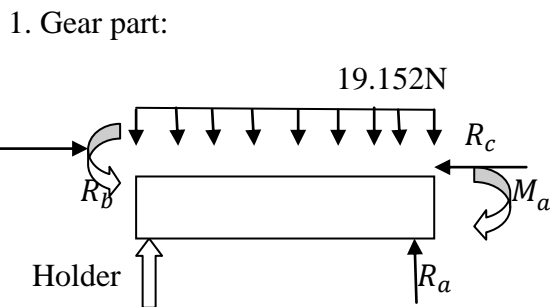
$$\text{ratio is} = 1:0.56$$

Therefore the force is in the ratio of

$$34.2 \times 0.56 = 19.152$$

$\therefore$  ratio is

$$49.248:19.152$$



$$\sum f_y = 0$$

$$\sum f_x = 0$$

$$\sum M_a = 0$$

$$R_a = (19.152 \times 0.037) + 1243 = 1951.62$$

$$m_{R_a} - (19.152 \times 0.037) \times 0.0185 - (1243 \times 0.037) = 0$$

$$m_{R_a} = 13.10 - 45.991$$

$$= -32.891 \downarrow N.m$$

$$R_c = 452.73 N.m$$

$$m_{R_c} = -452.73 \times 0.037 + R_c$$

$$= 16.75 N.m$$

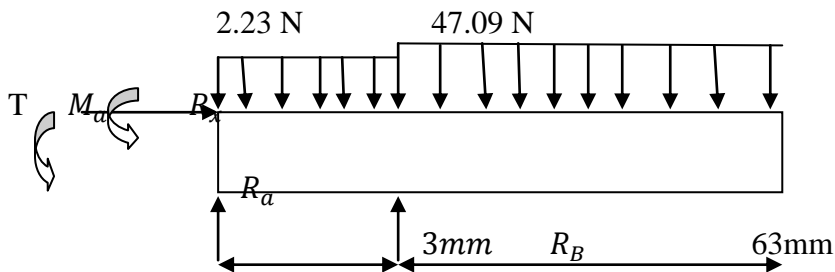
$$-M_a + (19.152 \times 0.037) \times 0.0185 + (1243 \times 0.037) + 61.65 = 0$$

$$M_a = 120.66 N.m$$

$$\therefore \sigma_x = \frac{120.66}{11.04}$$

$$= 10.92 N/mm^2$$

For wheel part:



$$\sum f_y = 0$$

$$\sum f_x = 0$$

$$\sum M_B = 0$$

$$R_x = 0$$

$$R_B + 1951.62 = 40 + (47.09 \times 0.063) + 2.23$$

$$R_B = 1056.7 N$$

$$61.56 - 120.66 - M_B - 1951.62 \times 0.003 + (2.23 \times 0.003 \times 0.0015) - (47.09 \times 0.063) \times 0.0315 = 0$$

$$M_B = -158.19 \leftarrow N.m$$

$$\begin{aligned} \therefore \sigma_x &= \frac{158.19}{28.27} \\ &= 5.59 \text{ N/mm}^2 \end{aligned}$$

#### 4.6.6 Twisting moment

$$M = \frac{\pi}{16} \times \tau \times d^3 \quad (31)$$

$$\begin{aligned} M_{gear} &= \frac{\pi}{16} \times 0.0928 \times 15^3 \\ &= 61.49 \end{aligned}$$

$$\begin{aligned} M_{wheel} &= \frac{\pi}{16} \times 0.022 \times 24^3 \\ &= 59.71 \end{aligned}$$

#### 4.6.7 Combined maximum shear stress

$$\tau = \left( \sigma_s^2 + \left( \frac{\sigma}{2} \right)^2 \right)^{1/2} \quad (32)$$

For gear part:

$$\begin{aligned} \tau_{max} &= 0.0928^2 + \left( \frac{0.046}{2} \right)^{1/2} \\ &= 0.095 \text{ N/mm}^2 \end{aligned}$$

For wheel part:

$$\begin{aligned} \tau_{max} &= 0.022^2 + \left( \frac{0.011}{2} \right)^{1/2} \\ &= 0.022677 \text{ N/mm}^2 \end{aligned}$$

#### 4.6.8 Maximum normal stress

$$\sigma_e = \frac{\sigma}{2} \pm \left( \sigma_s^2 + \left( \frac{\sigma}{2} \right)^2 \right)^{1/2} \quad (33)$$

For gear

$$\sigma_e = \frac{0.046}{2} + 0.095$$

$$= 0.11835 \text{ N/mm}^2$$

For wheel

$$\sigma_e = \frac{0.011}{2} + 0.0226$$

$$= 0.0281312 \text{ N/mm}^2$$

#### 4.6.9 Analysis of stress point critical section

##### a. gear shaft

$$\sigma_x = \frac{Mc}{I} + \frac{P}{area} \quad (36)$$

$$\sigma_x = \frac{Fl\left(\frac{d}{2}\right)}{I} + \frac{4P}{\pi d^2} \quad (37)$$

$$M = 120.66 - T$$

$$= 120.66 - 61.56$$

$$= 59.1 \text{ N.m}$$

$$\therefore \sigma_x = \frac{59.1}{11.04} \times \left(\frac{0.015}{2}\right) + \frac{452.73 \times 4}{\pi \times 0.015^2}$$

$$= 2602.07 \text{ kPa}$$

$$\tau_{xy} = \frac{Tr}{j} = \frac{16T}{\pi d^3} \quad (38)$$

$$= \frac{16 \times 61.56}{\pi \times 0.015^3}$$

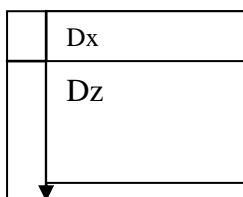
$$= 92895.5 \text{ kPa}$$

And now we can find von-misses stress

$$\sigma_{vm} = \sqrt{(\sigma_x^2 + 3\tau_{xy}^2)} \quad (39)$$

$$= 160.9207 \text{ MPa}$$

Point A at shaft:



$$\sigma_x = \sigma_A$$

$$\sigma_y = 0$$

$$\tau_{xy} = ?$$

$$\sigma_{1,2} = 0.5(\sigma_x + \sigma_y) \pm \sqrt{\frac{(\sigma_x - \sigma_y)^2}{2} + \tau_{xy}^2} \quad (40)$$

$$\sigma_{1,2} = 0.5(2602.07) \pm \sqrt{\frac{(2602.07)^2}{2} + 92895.5^2}$$

$$\sigma_1 = 94.20561 \text{ MPa}$$

$$\sigma_2 = 91.60361 \text{ MPa}$$

$$\tau_{max}, \tau_{min} = \pm 0.5 \sqrt{(\sigma_x)^2 + 4\tau_{xy}^2} \quad (41)$$

$$\tau_{max}, \tau_{min} = \pm 0.5 \sqrt{2602.07^2 + 4(92895.5)^2}$$

$$\tau_{max} = 92.90461 \text{ MPa}$$

$$\tau_{min} = -92.90461 \text{ MPa}$$

## B) Wheel shaft

$$\sigma_x = \frac{Mc}{I} + \frac{P}{area}$$

$$\sigma_x = \frac{F l \left(\frac{d}{2}\right)}{I} + \frac{4P}{\pi d^2}$$

$$158.19 - T$$

$$158.19 - 61.56$$

$$123.63 \text{ N.m}$$

$$\therefore \sigma_x = \frac{123.63}{28.27} \times \left(\frac{0.024}{2}\right) + \frac{452.73 \times 4}{\pi \times 0.024^2}$$

$$= 1000.7 \text{ kPa}$$

$$\tau_{xy} = \frac{T r}{j} = \frac{16T}{\pi d^3}$$



$$= \frac{16 \times 61.56}{\pi \times 0.024^3}$$

$$= 22679.5 \text{ kPa}$$

$$\sigma_{vm} = \sqrt{(\sigma_x^2 + 3\tau_{xy}^2)}$$

$$= 124.261 \text{ MPa}$$

Point A at shaft:

	$D_x$
	$D_z$

$$\sigma_x = \sigma_A$$

$$\sigma_y = 0$$

$$\tau_{xy} = ?$$

$$\sigma_{1,2} = 0.5(\sigma_x + \sigma_y) \pm \sqrt{\frac{(\sigma_x - \sigma_y)^2}{2} + \tau_{xy}^2}$$

$$\sigma_{1,2} = 0.5(1000.7) \pm \sqrt{\frac{(1000.70)^2}{2} + 22679.5^2}$$

$$\sigma_1 = 23.19088 \text{ MPa}$$

$$\sigma_2 = 22.19018 \text{ MPa}$$

$$\tau_{max}, \tau_{min} = \pm 0.5 \sqrt{(\sigma_x)^2 + 4\tau_{xy}^2}$$

$$\tau_{max}, \tau_{min} = \pm 0.5 \sqrt{1000.7^2 + 4(22679.5)^2}$$

$$\tau_{max} = 22.68501 \text{ MPa}$$

$$\tau_{max} = -22.68501 \text{ MPa}$$

## 4.7 Material selection

Material selection is a step in the process of designing any physical object. In the context of product design, the main goal of material selection is to minimize cost while meeting product

performance goals. Systematic selection of the best material for a given application begins with properties and costs of candidate materials.

### **4.7.1 Frame and body holder material**

The type of material used to construct the frame affects the weight of the frame, and therefore the overall weight of the wheelchair. The type of frame material also can affect the wheelchair's overall strength.

#### **4.7.1.1 Mild Steel**

Mild steel, also called as plain-carbon steel, is the most common form of steel because its price is relatively low while it provides material properties that are acceptable for many applications, more so than iron. Low-carbon steel contains approximately 0.05–0.3% carbon making it malleable and ductile. For mild steel  $\sigma = 580\text{N/mm}^2$

#### **4.7.1.2 Aluminum**

is remarkable for the metal's low density and its ability to resist corrosion through the phenomenon of passivation. Aluminum and its alloys are vital to the aerospace industry and important in transportation and building industries, such as building facades and window frames. The oxides and sulfates are the most useful compounds of aluminum. Aluminum has about one-third the density and stiffness of steel. It is easily machined, cast, drawn and extruded.

#### **4.7.1.3 Stainless steel**

is a steel alloy with a minimum of 10.5% chromium content by mass. It is notable for its corrosion resistance, Stainless steel does not readily corrode, and rust or stain with water as ordinary steel does. However, it is not fully stain-proof in low-oxygen, high-salinity, or poor air-circulation environments.

### **4.7.2 Type of Wheel/Tires Material**

#### **4.7.2.1 Filled rubbers**

In tires rubbers are usually filled with particles like carbon black or Silica. They consist of a tread and a body. The tread is the part of the tire that comes in contact with the road surface. The portion that is in contact with the road at a given instant in time is the contact.

### 4.7.2.2 Polyurethane

Polyurethane (PUR and PU) is a polymer composed of a chain of organic units joined by carbonate (urethane) links. The main ingredients to make polyurethane are isocyanides. Other materials are added to help processing the polymer or to change the properties of the polymer.

### 4.7.2.3 Steel

Steel is an alloy of iron, with carbon being the primary alloying element, up to 2.1% by weight. Various Wheel materials and their co-efficient of frictions are tabulated in table 3.3.

**Table 0.2: Various Wheel Materials and their Coefficient of friction**

S.NO	Material	Coefficient of friction
1	Rubber concrete	0.85
2	Polyurethane concrete	0.5
3	Steel concrete	0.45

The wheels are of rubber as it has to bear the whole load of the person sitting in the chair and has the highest Coefficient of friction.

### 4.7.3 Shaft materials

Most shafts are made from steel, either low- or medium-carbon. However, high quality alloy steel, usually heat treated, may be chosen for critical applications.

Other metals, e.g. brass, stainless steel or aluminum, may be used where corrosion is a problem or lightness is required.

# Chapter Five

## Results and Discussion

### 5.1 Introduction

This chapter presents the findings from tri-star wheel frame analysis using aluminum, stainless steel and mild steel, the description of the final design and discusses both mathematical and simulation analysis results.

### 5.2 Tri-wheel holder system analysis

This part of chapter provides an overview of results obtained from static force applied on model using solid work, results presented includes( von misses stress, von misses strain and displacement occurred).

#### 5.2.1 Material of holder

Materials conducted in the analysis were based on material selection study introduced in (chapter 4).

##### 5.2.1.1 Aluminum

The detected results are presented in table below

**Table 0.1: Max stress, strain and displacement of aluminium**

Max. stress	Max. strain	Max. displacement	Deformation scale
$6.281 \times 10^5$	$1.053 \times 10^{-6}$	$1.883 \times 10^{-3}$	25454

##### 5.2.1.2 Stainless steel frame

The detected results are presented in table below

**Table 0.2: Max stress, strain and displacement of stainless steel**

Max. stress	Max. strain	Max. displacement	Deformation scale
$4.256 \times 10^5$	$1.426 \times 10^{-6}$	$2.837 \times 10^{-3}$	16875.4

##### 5.2.1.3 Mild-steel frame

The detected results are presented in table below

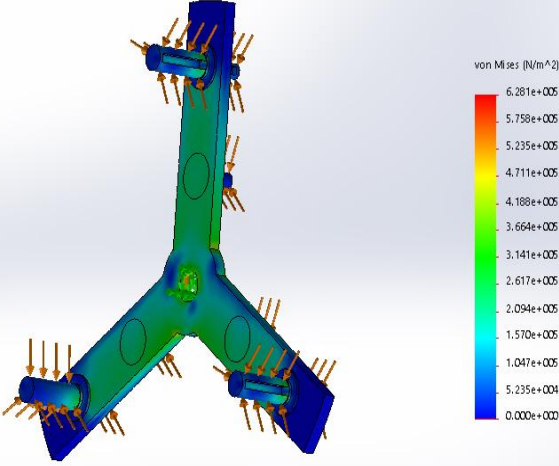
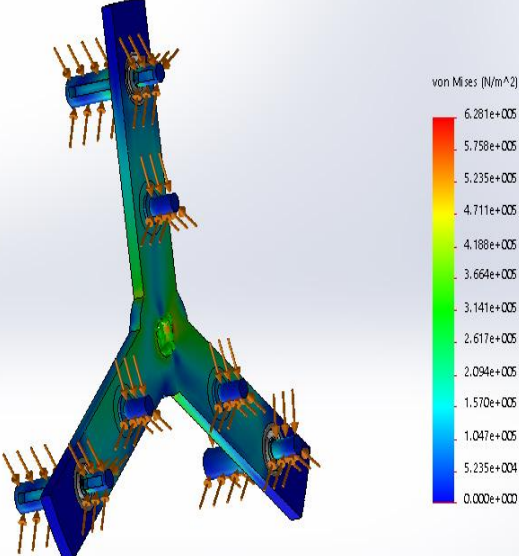
**Table 0.3: Max stress, strain and displacement of mild steel**

Max. stress	Max. strain	Max. displacement	Deformation scale
$4.281 \times 10^5$	$1.362 \times 10^{-6}$	$2.755 \times 10^{-3}$	1

### 5.2.2 Von misses stress

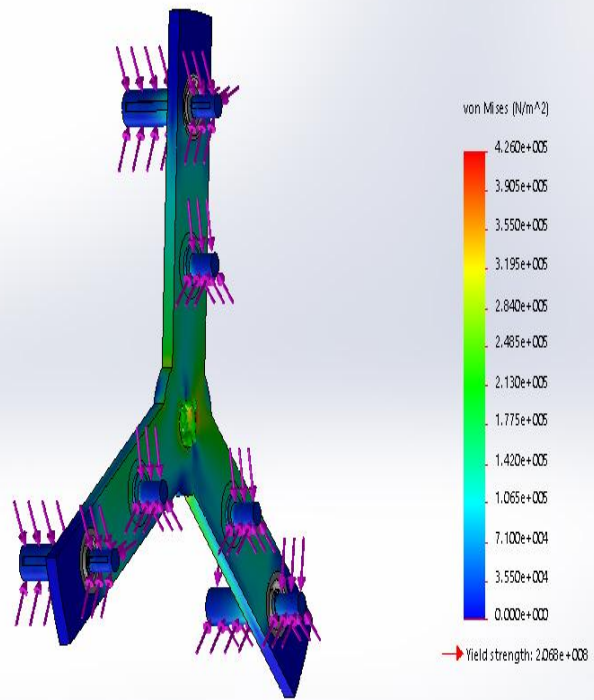
The following table shows equivalent von misses stress distribution in the frame with the different material selected.

**Table 0.4: Von misses stress distribution**

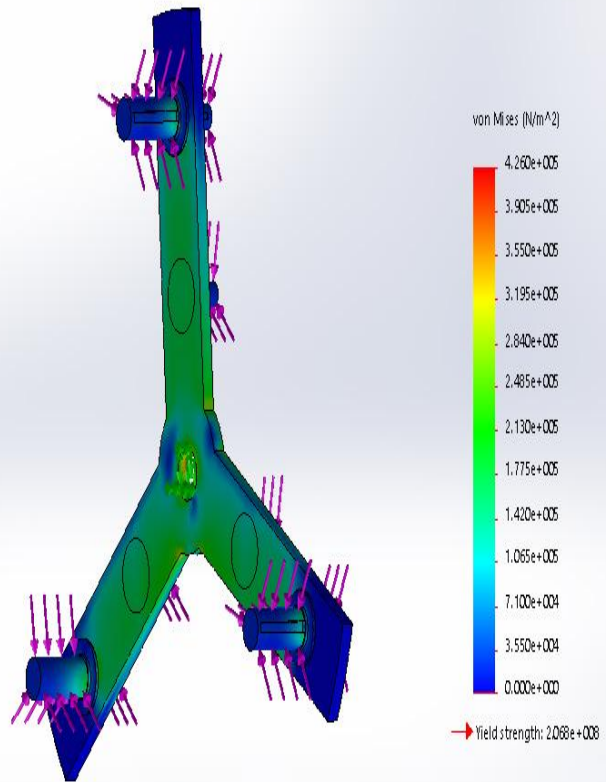
material	Von misses stress distribution
Aluminum	<div data-bbox="427 678 603 728" style="border: 1px solid black; padding: 2px; font-size: small;">                     Model nameholder with 2 \$rafts                      Study name:Static 4(-Default-)                      Plot type: Static nodal stress: Stress1                 </div>  <div data-bbox="427 1308 603 1357" style="border: 1px solid black; padding: 2px; font-size: small;">                     Model nameholder with 2 \$rafts                      Study name:Static 4(-Default-)                      Plot type: Static nodal stress: Stress1                 </div> 

# Stainless steel

Model name:holder with 2 \$afts  
Study name:static 2(-Default-)  
Plot type:Static nodal stress Stress1

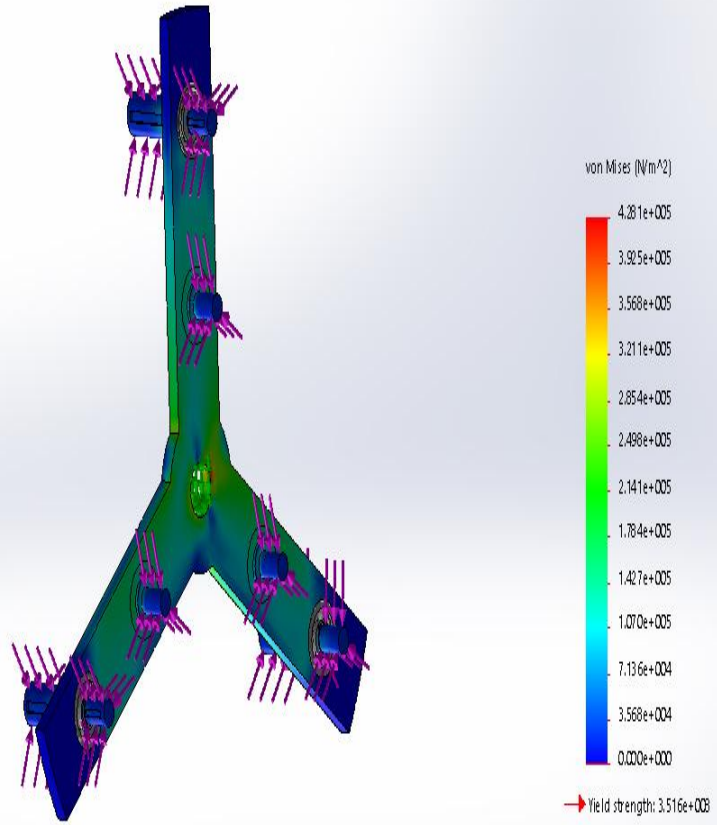


Model name:holder with 2 \$afts  
Study name:static 2(-Default-)  
Plot type:Static nodal stress Stress1

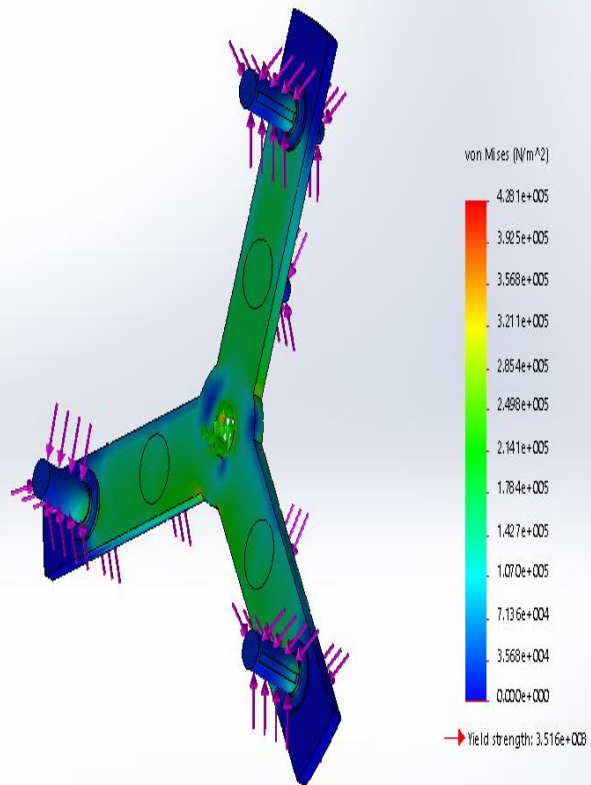


# Mild steel

Model name:holder with 2 shafts  
Study name:Static 3(-Default-)  
Plot type:Static nodal stress: Stress1



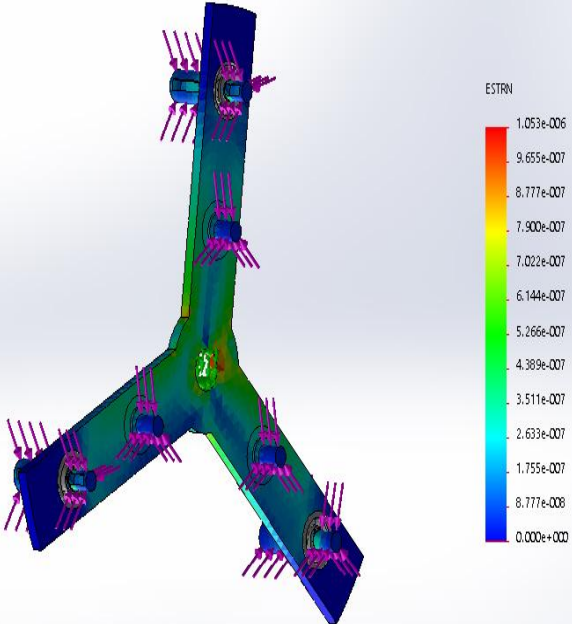
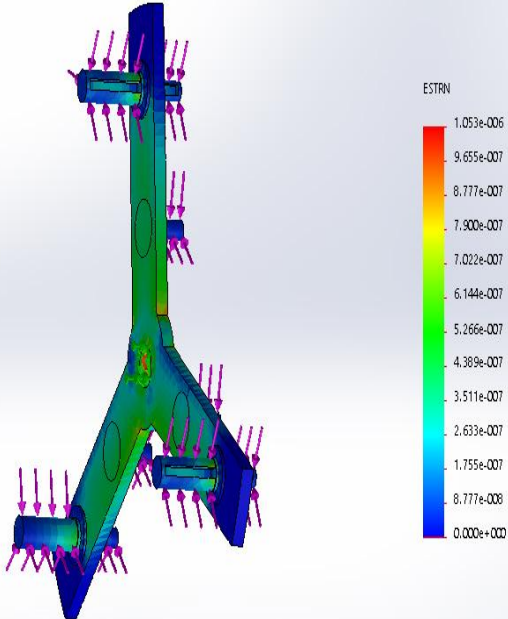
Model name:holder with 2 shafts  
Study name:Static 3(-Default-)  
Plot type:Static nodal stress: Stress1



### 5.2.3 Von-misses strain

The following table shows equivalent von misses strain distribution in the frame with the different material selected.

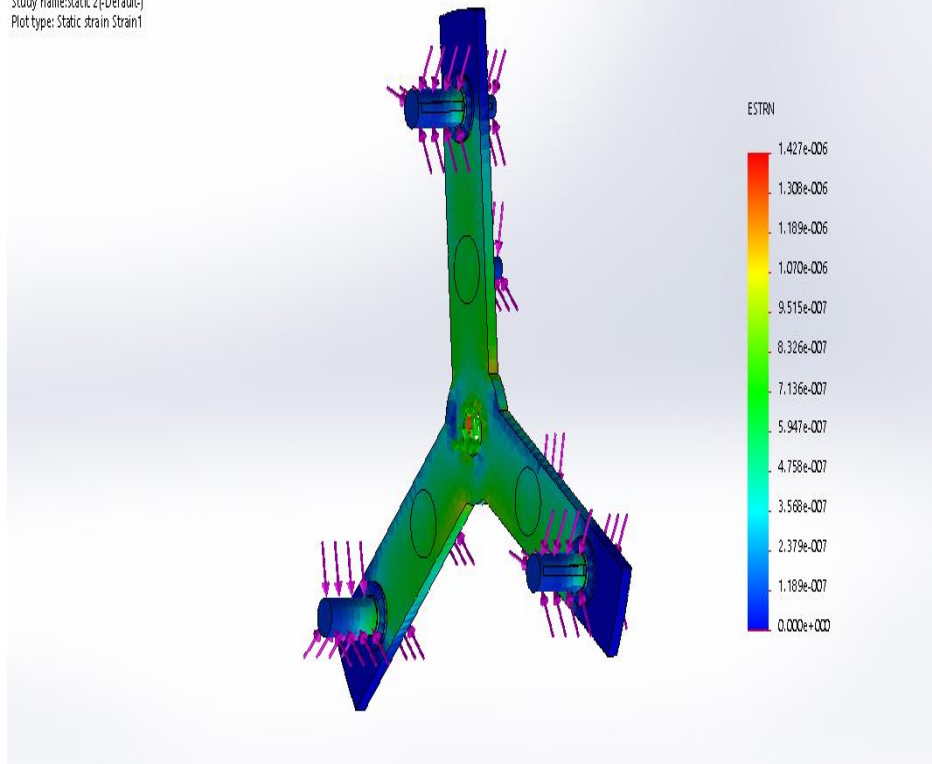
**Table 0.5: Von-misses strain distribution**

material	Von-misses strain distribution
<p>Aluminum</p>	<div style="display: flex; flex-direction: column; align-items: center;"> <div style="margin-bottom: 20px;"> <p>Model nameholder with 2 \$fafts Study name:Static 4(-Default-) Plot type: Static strain Strain1</p>  </div> <div> <p>Model nameholder with 2 \$fafts Study name:Static 4(-Default-) Plot type: Static strain strain1</p>  </div> </div>

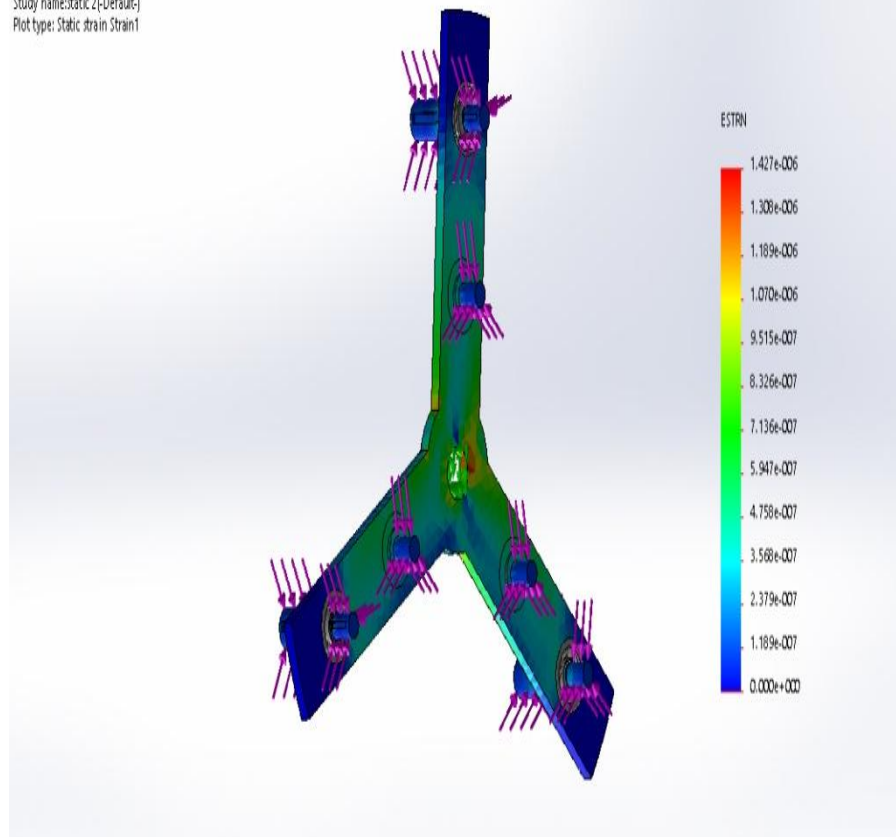


# Stainless steel

Model nameholder with 2 \$fts  
Study name:static 2(-Default-)  
Plot type: Static strain Strain1

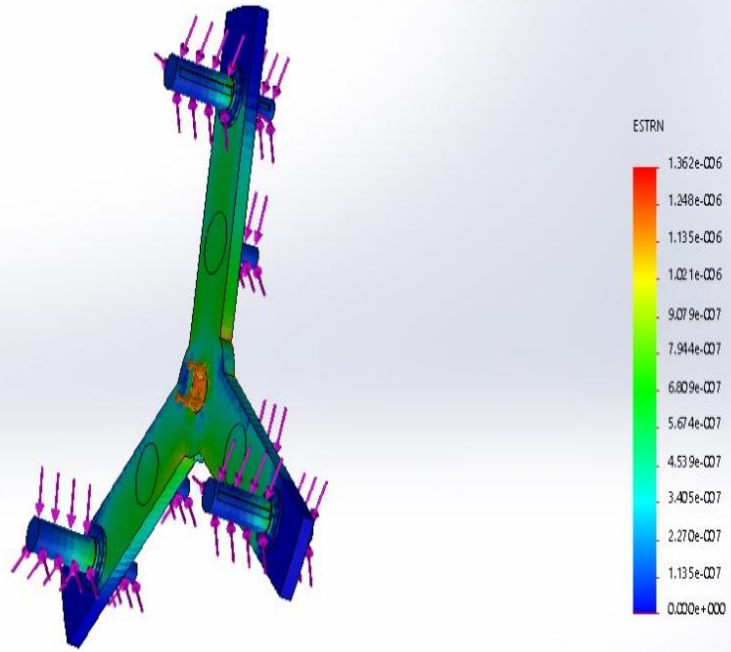


Model nameholder with 2 \$fts  
Study name:static 2(-Default-)  
Plot type: Static strain Strain1

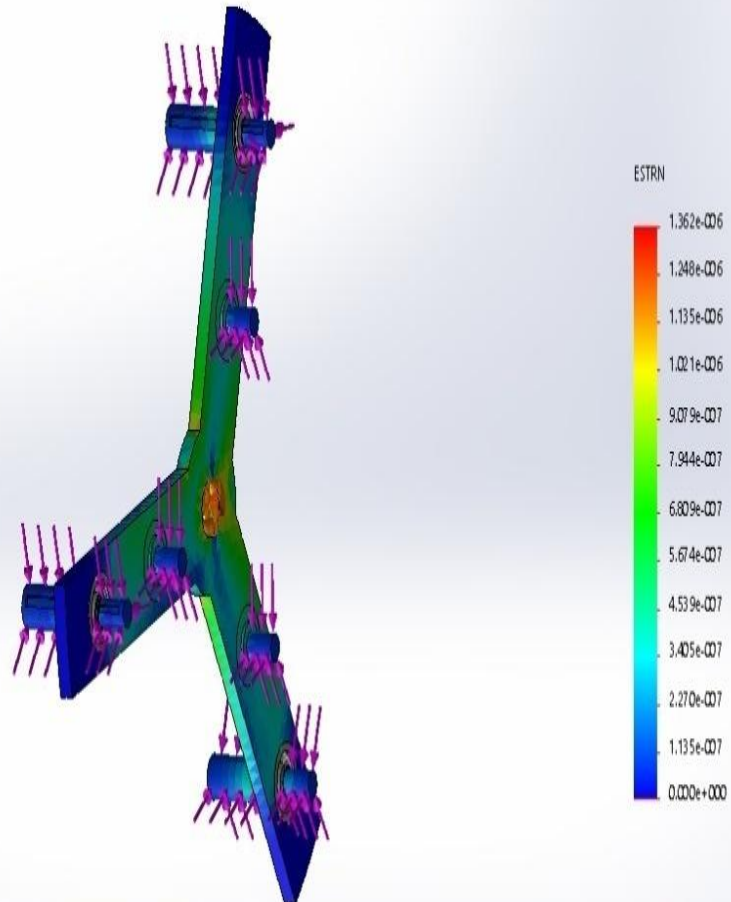


# Mild steel

Model name: holder with 2 shafts  
Study name: Static 3 (Default-)  
Plot type: Static strain Strain1



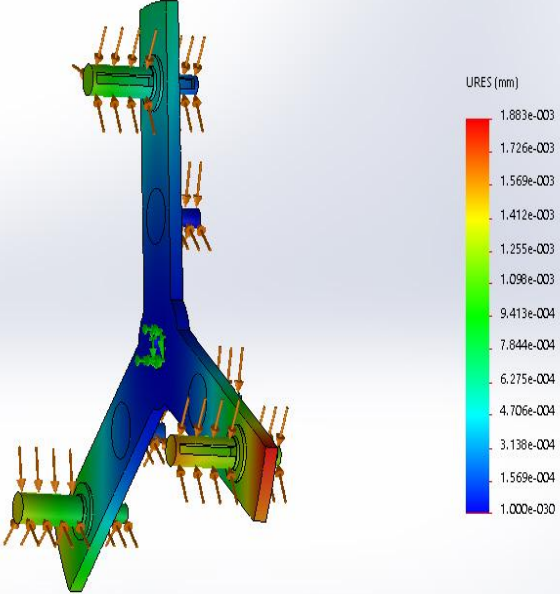
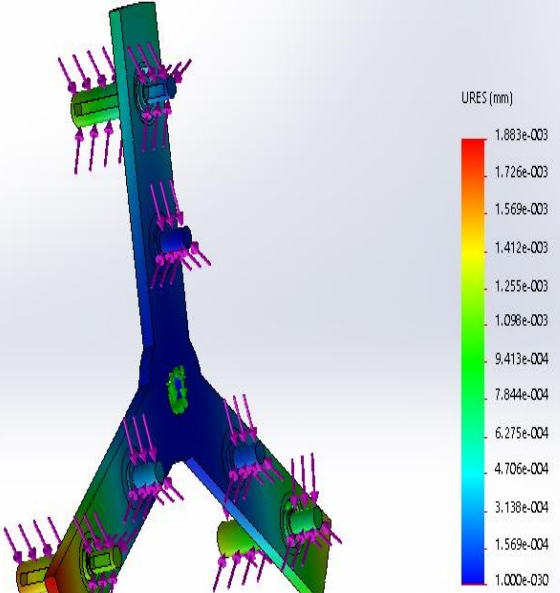
Model name: holder with 2 shafts  
Study name: Static 3 (Default-)  
Plot type: Static strain Strain1



## 5.2.4 Displacement

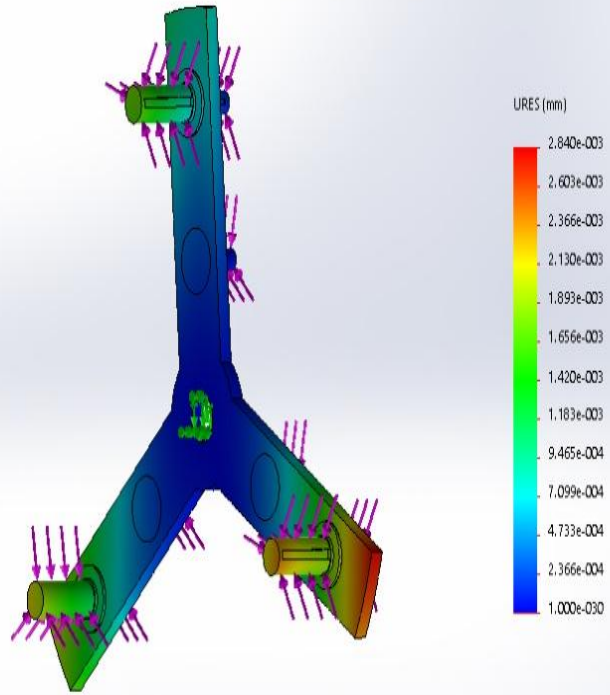
The following table shows displacement distribution in the frame with the different material selected.

**Table 0.6: Displacement distribution**

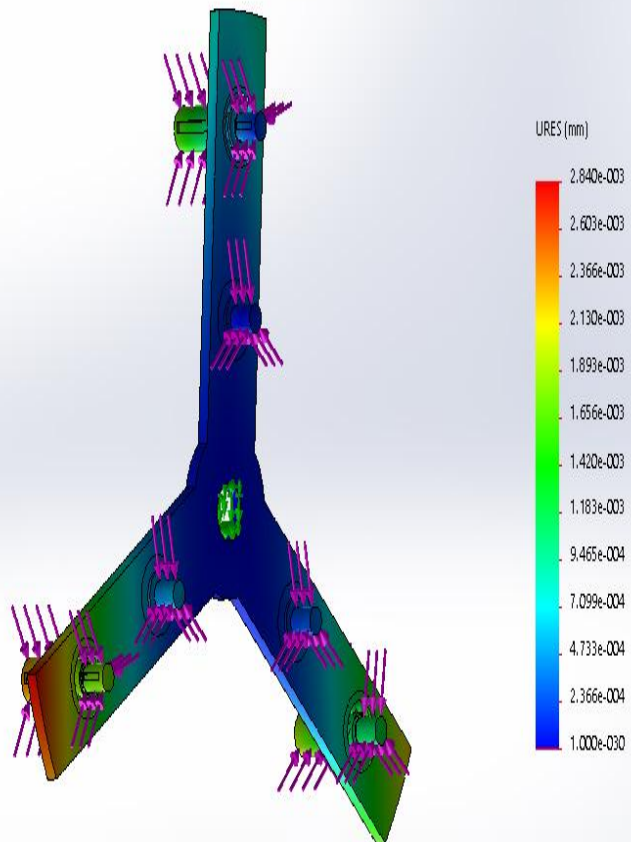
material	Displacement distribution
<p>aluminum</p>	<div style="display: flex; flex-direction: column; align-items: center;"> <div style="display: flex; justify-content: space-between; width: 100%;"> <span data-bbox="391 568 619 622">Model nameholder with 2 \$afts Study name:Static 4(-Default-) Plot type: Static displacement Displacement1</span>  </div> <div style="display: flex; justify-content: space-between; width: 100%; margin-top: 20px;"> <span data-bbox="391 1258 628 1312">Model nameholder with 2 \$afts Study name:Static 4(-Default-) Plot type: Static displacement Displacement1</span>  </div> </div>

Stainless  
steel

Model nameholder with 2 \$afts  
Study name:static 2(-Default-)  
Plot type: Static displacement Displacement1

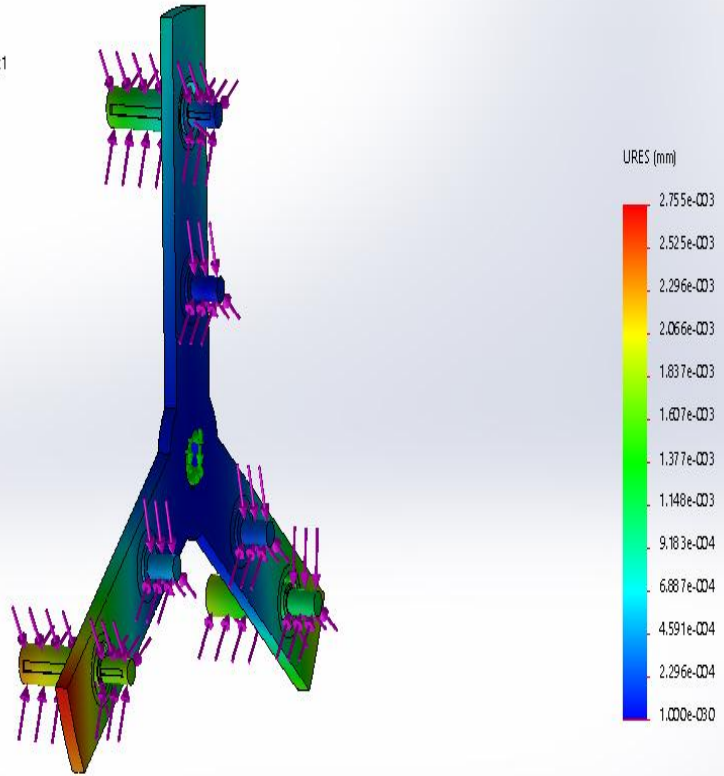


Model nameholder with 2 \$afts  
Study name:static 2(-Default-)  
Plot type: Static displacement Displacement1

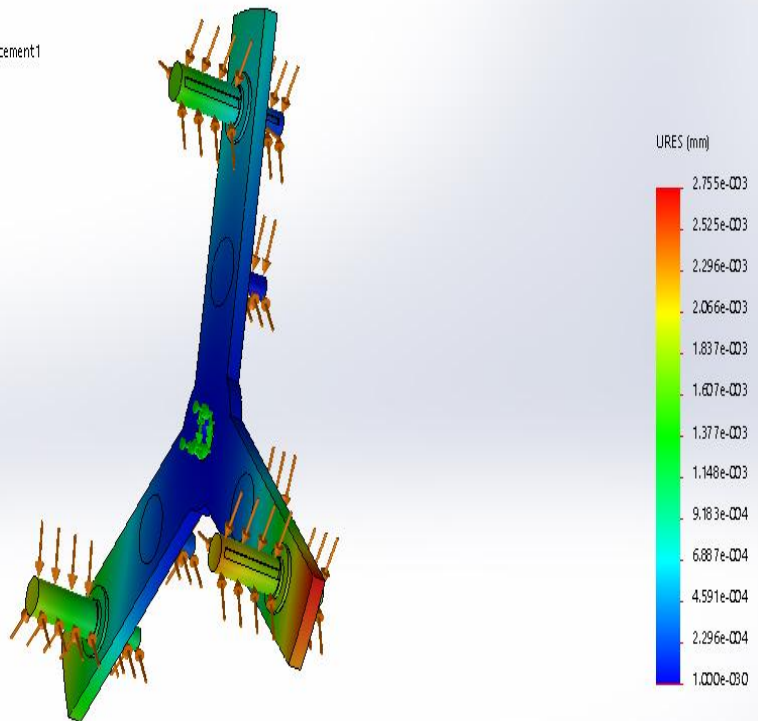


## Mild steel

Model name: holder with 2 shafts  
Study name: Static 3 (Default)  
Plot type: Static displacement Displacement1



Model name: holder with 2 shafts  
Study name: Static 3 (Default)  
Plot type: Static displacement Displacement1



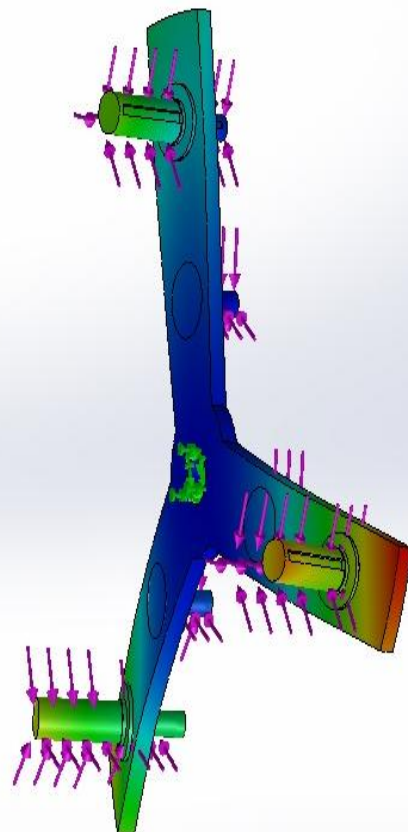
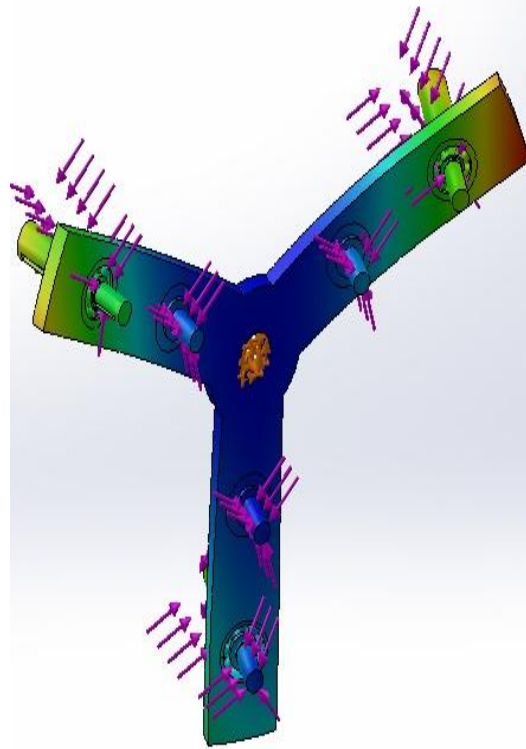
## 5.2.5 Deformation

The following table shows deformation occurred within the frame by the different material selected.

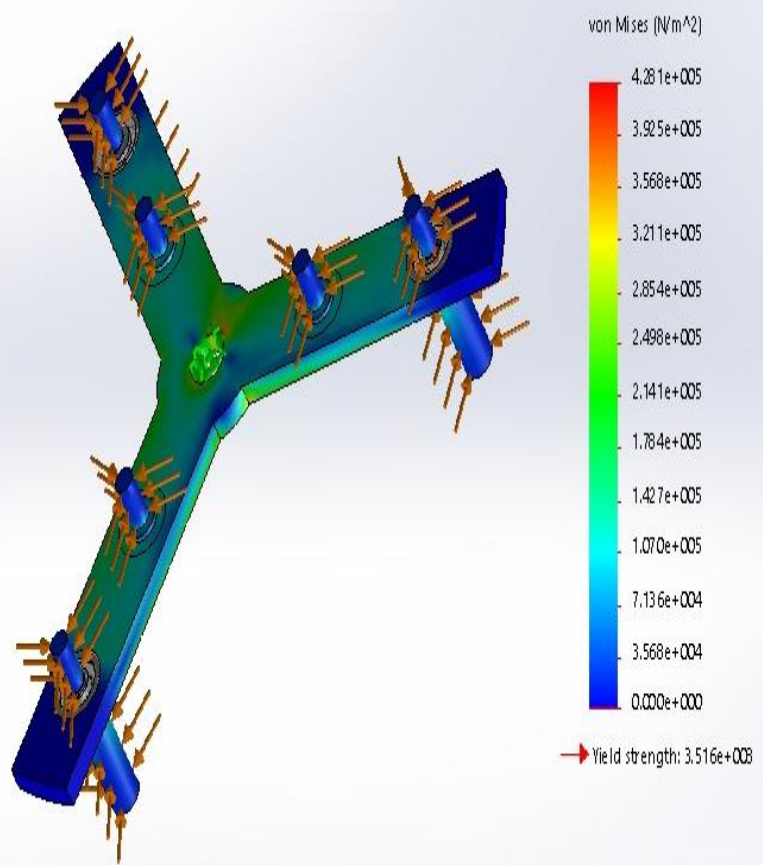
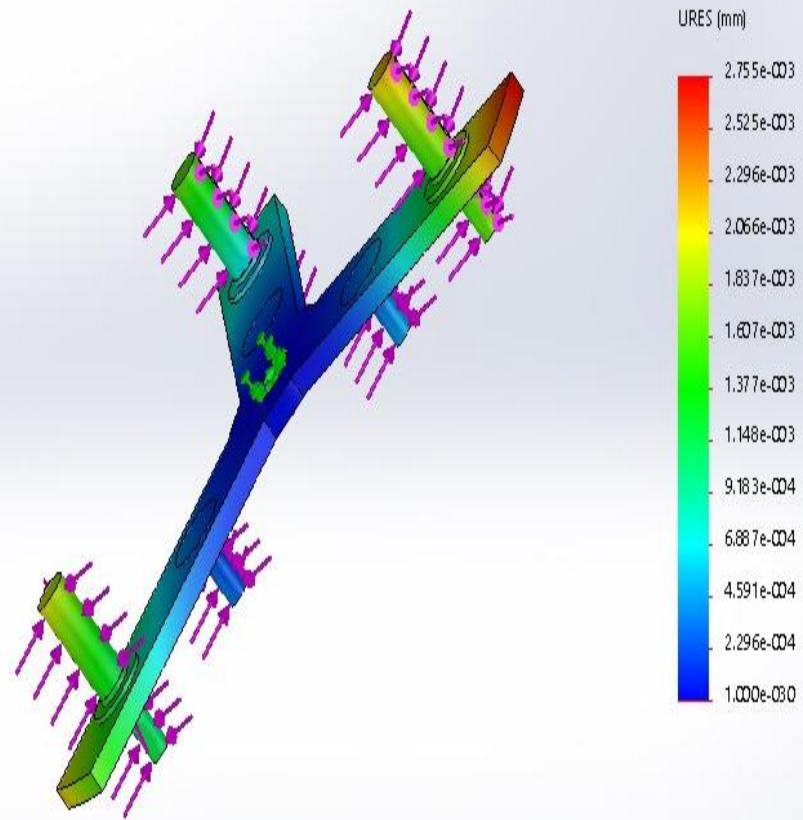
**Table 0.7: The Resultant Deformation**

Material	deformation
aluminum	<p>The figure displays two 3D FEA plots of a Y-junction frame. The top plot, labeled 'ESTRN', shows the effective strain distribution across the frame. The color scale ranges from 0.000e+000 (blue) to 1.053e-006 (red). The bottom plot, labeled 'URES (mm)', shows the effective displacement distribution. The color scale ranges from 1.000e-030 (blue) to 1.883e-003 (red). Both plots include pink arrows indicating the direction of applied loads.</p>

Stainless steel



Mild steel





### 5.3 Final Design

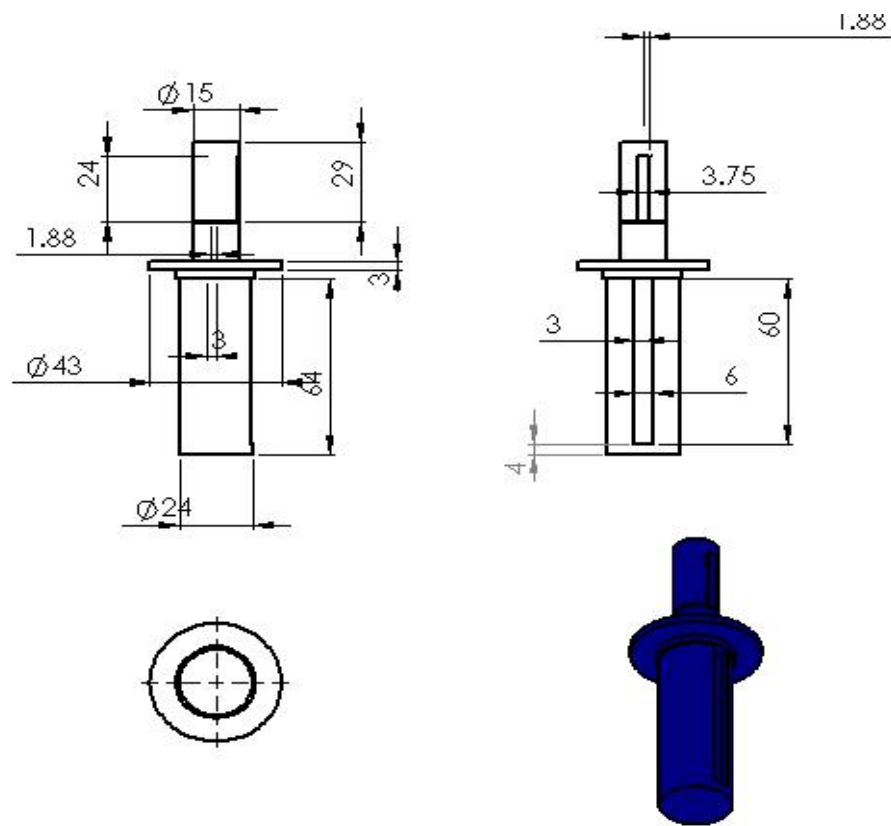


Figure 5.1: Final shaft

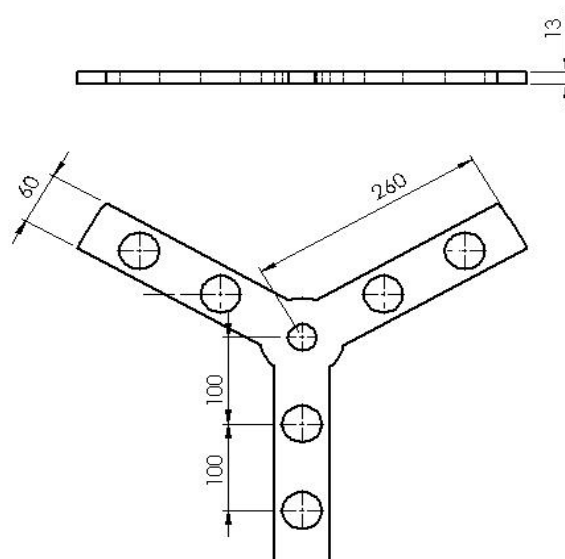


Figure 5.2: holder

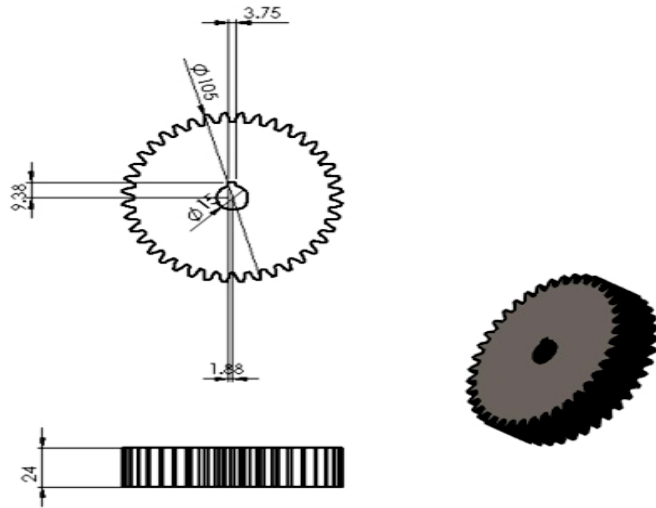


Figure 5.3: gear with key seat

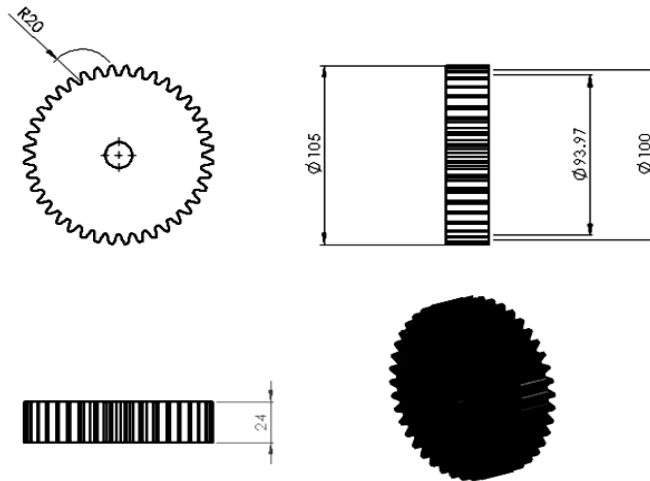


Figure 5.4: middle gear

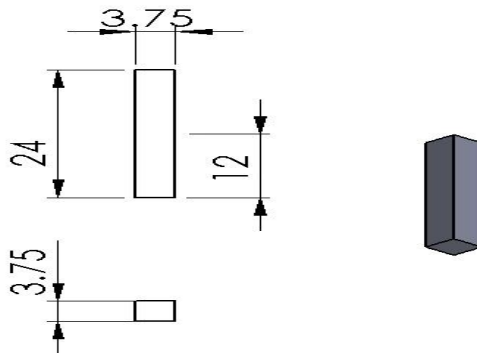


Figure 5.5: gear's key seat

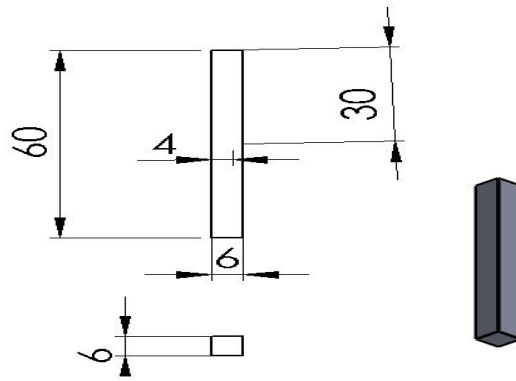


Figure 5.6: wheel's key seat

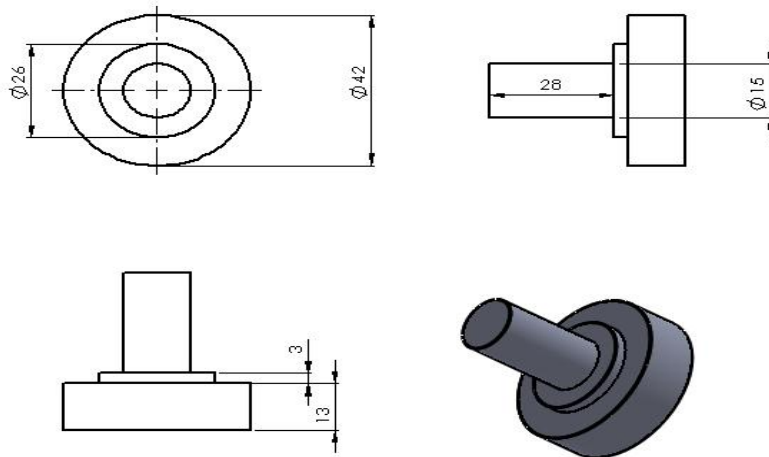


Figure 5.7: middle shaft

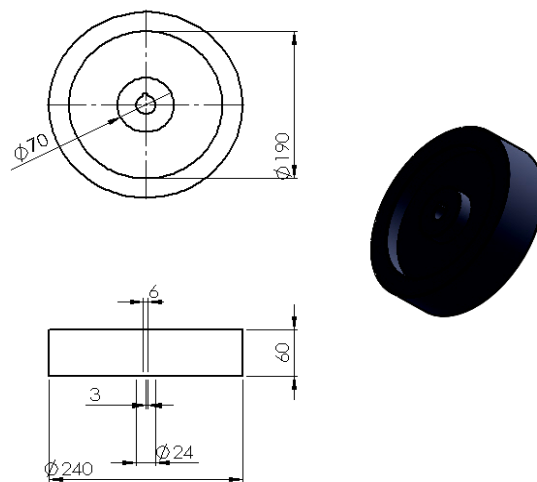


Figure 5.8: wheel

NO.	Component name
1	Tri-star wheel system
2	DC motor
3	Frame

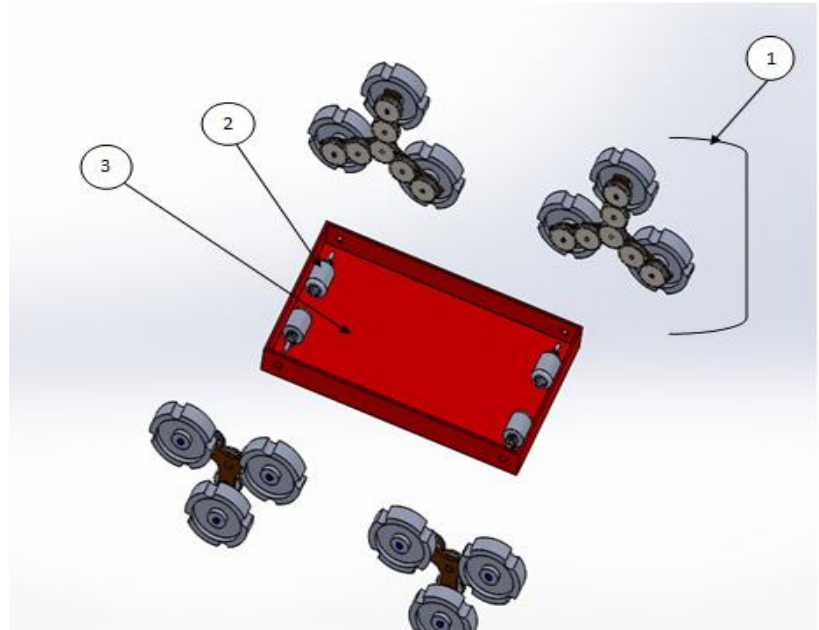


Figure 5.9: final system design

NO.	Name
1	Wheel
2	Wheel & gear Shaft
3	middle gears shaft
4	Holder
5	Bearing
6	Gears with key seat
7	Middle gear

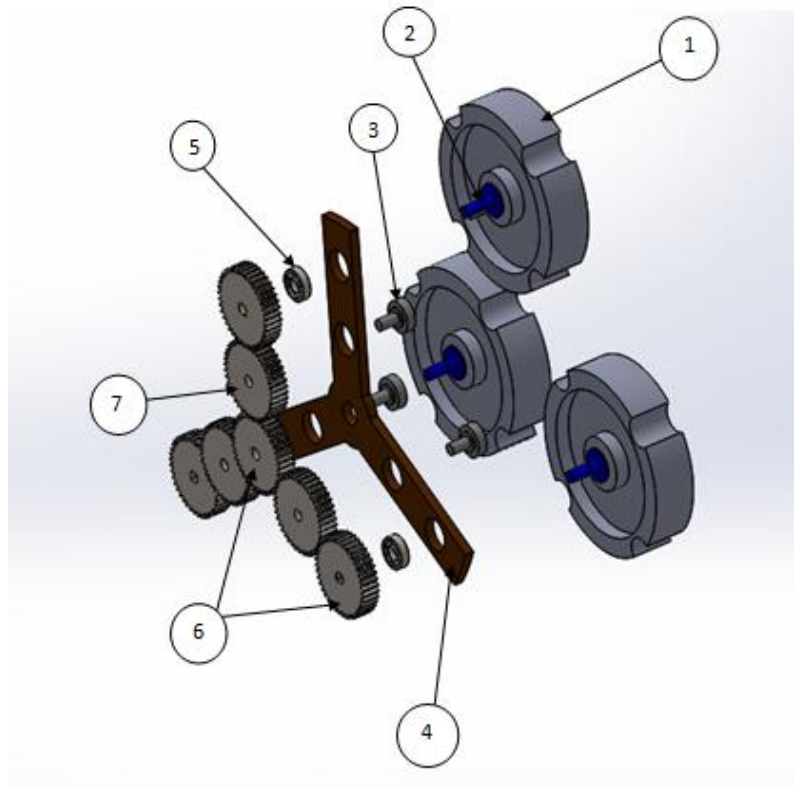


Figure 5.10: tri star wheel design

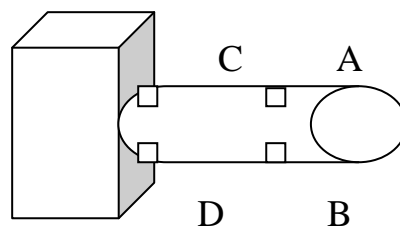
## 5.4 Discussion

Based on the calculated weights driven for the system The DC motor was chosen to provide high torque to bear the calculated load exerted on the system and low speed to maintain stability.

The presented terms of operation led to chose gear system for transmission due to its Small amount of friction, less chance of slipping, capability of transmitting high torque, High efficiency and Quietness.

From the obtained results there had been two types of stresses Normal stress which was caused by the forces exerted by 90 degree on the system and Shear stress which was parallel to the system normal stress was caused by two forces, axial and bending. Axial Resulted from total pulling force exerted on the system for motion, it was equal along the shaft and bending Resulted from the exerted force by wheel, gear and weight of system. It appeared at the top and bottom of the shaft where they exhibited compression and tension respectively.

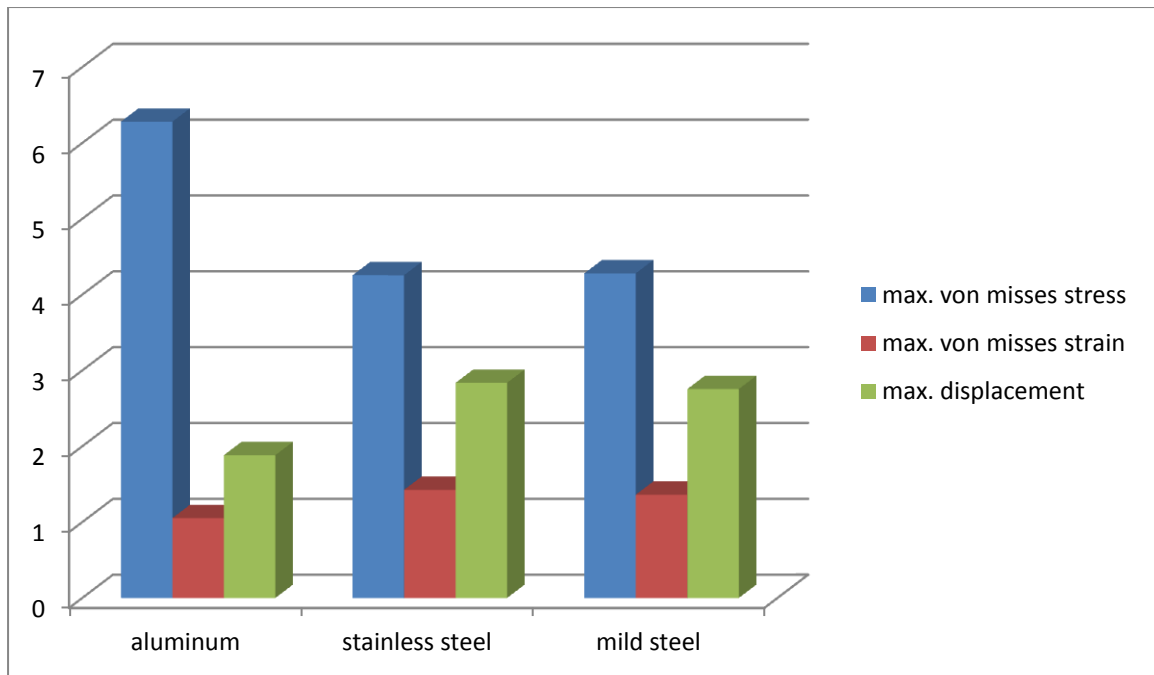
Shear stress was caused by two forces Transverse and torsion. Transverse force Caused the shear stress to be maximum at center in both sides of the shaft (left and right of the load) due to the reaction forces at both ends of the shaft .The torsion shear stress was most high at wheel part of the shaft than gear part due to its large area were the torsion is proportional to it. And by further more the element around the outside parameter (i.e. points A and B) exhibited the maximum shear stress due to torsion which increase when the distance (i.e. moment arm) increase.



**Figure 5.11: shaft stress points**

The normal stresses due to bending are largest at the cross section of maximum bending moment, which is at the support as shown above (i.e. at points C and D). Specifying the procured results with the chosen material (mild steel, stainless steel and aluminum) the following points were found.

Von misses Stress presented along the shaft were at most towards the fixed end of beam which is less than the yield point value of mild steel Aluminum and Stainless steel therefore, the design is safe in all nevertheless, from the analysis done with the three materials results showed that mild steel deformation is best of the three due to it's high ductility beside its less cheaper than both of them. Even though in relative to stainless steel and aluminum it had lower strength and hardness. Above that aluminum took the prize for light weight.



**Figure 5.12: Max stress, strain and displacement for the 3 material**

# **Chapter Six**

## **Conclusions and Recommendations**

### **6.1 Conclusions**

This project aimed to develop a mechanism for climbing stair using tri-star wheel system which its main idea was making the wheels rolling within motion in flat surfaces while in climbing motion the whole system will roll together. Gear system was chosen as transmission system. A mechanical design simulation and analysis were presented using SOLIDWORK program. The first model was inefficient due to it's incompatibility with dynamic running therefore, it was modified. In particular it's the gear and wheel shaft was modified to shaft composed of two portions with different areas and bearing was added to prevent holder's motion with that shaft. In the other side the key seats had been added to transmit power from the gear to the shaft then to the wheel.

For analysis aluminum, stainless steel and mild steel were used to test the best behavior of design with it. Though the three materials provided tolerated results, mild steel wins the first place in terms of cost, weight and ductility.

### **6.2 Recommendation**

With the evolution of computers in terms of programs, speed and accuracy the design performance simulation and analysis can be done with such software programs. The design here was analyzed in static position with high loads in static analysis so, further research may contain an experimental tests with load resulted from the climbing motion.

In terms of safety future research can add clutch, a mechanical device which engages and disengages power transmission from driving shaft to driven shaft. Also with this huge transition in modern technologies future research can implement collision avoidance mechanism using ultrasonic sensors and switches for controlling various operation modes of the system.

## References

- [1] "why population aging matters: A global prespective," 13 march 2011. [Online]. Available: <http://www.globalization101.org/world-report-on-disability-3/>. [Accessed 3 december 2016].
- [2] m. a. majid m. moghaddam, *bioinspiration and robotics: walking and climbing robots*, vienna : i-tech, 2014.
- [3] "wheelchair ramp information," northeast rehabilitation hospital network, [Online]. Available: <http://www.northeastrehab.com/articles/ramps.htm..> [Accessed 17 june 2017].
- [4] g. a. m.ceccarelli, "climbing stairs with EPWAR2 biped robot," in *IEEE international confrence on robotics and automation (ICRA)*, Seoul, 2001.
- [5] y. w. a. b. l. j. liu, "analysis of stairs climbing ability for a tracked reconfigurable modular robot," in *IEEE international workshop on safty, security and rescue robotics* , kobo , 2005.
- [6] h. k. shashank shekar sahuo et al., "research on optimization, dynamics and stability of stair climbing wheelchair," *international journal of engineering research and application* , vol. 6, no. 3, pp. 74 - 79, 2016.
- [7] C. S. Birk A, "Rescue robotics a crucial milestone on the road to autonomous systems," *advanced robotic journal* , vol. 5, no. 20, pp. 595 - 576, 2017.
- [8] T. s. M. lawn, "modeling of a stair-climbing wheelchair mechanism with high single-step capablity," *IEEE transactions on neural systems and rehabilitation engineering*, vol. 11, no. 3, pp. 323 - 332, 2013.
- [9] H. S. O. R. A. H. L. H. S. T. T. O. B. S. Robarts J, "multi disciplinary engineering and business third year group mini-project, IPD labrotaries module," cork insitute of technology, 2012.



- [10] D. Y. B. C. Sandeep H.Deshmukh, "Development of stair climbing transporter," in *13th National Conference on mechanisms and machines (NACOMM07)*, Bangalore, 2007.
- [11] W. F. M. N. P. D. T. G. Quaglia, "Evaluation of wheelchair.Q, A stair climbing wheelchair," in *The 14th IFTOMM Congress*, Taipei, 2015.
- [12] F. V. G. A. P. a. P. Morales R., "Coordinated Motion of a new staircase Climbing Wheelchair with increased passenger comfort," in *International Conference on Robotics and Automation* , Florida, 2006.
- [13] Y. N. K. K. Sugahara Y., "A Novel Stair-Climbing Wheelchair with Transformable Wheeled Four-Bar Linkages," in *International Conference on Intelligent Robots and Systems* , Taipei, 2010.
- [14] H. S. Yuan j., "Research on leg-wheel Hybrid Stair-Climbing Robot," in *International Conference on Robotics and biomimetics*, Shenyang, 2004.
- [15] K. P. P. R. P. S. S. k. A. S. R. Rajasekar, "Design and Fabrication of Staircase Climbing Wheelchair," *International Journal of Mechanical Engineering and Robotic Research*, vol. 2, no. 2, pp. 320 - 323, 2013.
- [16] J. P. S. Dakamalla Shanmukh Anirudh, Design of Motorized Wheelchair, Rourkela: Department of Industrial Design National Institute of Technology, 2014.
- [17] S. K. C. A. S Shriwaskar, "Synthesis, Modeling, Analysis and Simulation of stair Climbing Mechanism," *International Journal of Mechanical Engineering and Robotics* , vol. 2, no. 4, pp. 0149 - 2278, 2013.
- [18] J. E. M. C. R. Shigley, Mechanical Engineering Design, McGraw Hill, 2001.
- [19] R. C. Juvinall, Fundamentals of Machine Component Design, Wiley, 1983.
- [20] *Bearing Self Study Guide*, USA: SKF Group , 2008.

- [21] NTN Corporate, *Bearing unite*(CAT. NO. 2400-IX/E), Illinois: New Technology Network (NTN), 2010.
- [22] E. H. I. I. J. S. M. S. Mohammad Iqbal, "MECHANICAL DESIGN AND DEVELOPMENT OF TRI-STAR WHEEL SYSTEM FOR STAIR CLIMBING ROBOT," in *Aceh Development International Conference*, Kuala Lumpur, 2012.
- [23] L. K. Hei, "Design and manufacture of stair climber," The Hong Kong Polytechnic University Industrial Centre , Hong Kong, 2012.
- [24] X. F. Lin Zhang, *An optimization Design for the Stair-Climbing Wheelchair*, Karlskrona, Sweden: Blekinge Institute of Technology, 2012.
- [25] "Staircase Design," in *National Building Code*, India, Public Buildings, 1983.
- [26] J. D. Irwin, *Mechanical Engineer's Handbook*, Auburn University, 2001.
- [27] C. R. JOHN BIRD, *Mechanical Engineering Principles*, Oxford: Reed Educational and Professional Publishing Ltd , 2002.
- [28] *Mechanical design manual*, Machinery Industry Press, 2007.

# Appendix A

To correctly design and dimension the boundary to the rotating system (bearing, houses etc.)  
The axial stress is calculated according to equation, and is normally comparatively small [27].

## 1. Normal stress

used to calculate forces exerted by 90degree on the system by the following equation

$$\sigma = \frac{F}{A} \quad (19)$$

Where,

$\sigma$  = Normal stress

F =pulling force

A= area

$$\text{area} = 2\pi r^2 + h(2\pi r) \quad (20)$$

r= radius

h = height of cylindrical shaft

## 2. Torsion shear stress

The resultant stress from torque applied on the shaft. Identified by the following equation

$$\sigma_s = \frac{T.D}{j} \quad (21)$$

Where,

$\sigma_s$  = Torsion shear stress

T= torque

J= shear constant(polar moment of inertia)

d= diameter of the shaft

$$j = \frac{\pi D^4}{32} \quad (22)$$
$$\therefore \sigma_s = T.D \times \frac{32}{\pi D^4}$$

$$\therefore \sigma_s = \frac{T}{a} \quad (23)$$

### 3. Load at the spur gear pitch circle

Is the load resulted from the torque applied on the spur gear pitch circle.

$$F_t = \frac{2T}{D_p} = \frac{2P \times 63,000}{D_p n} \quad (24)$$

Where,

$F_t$  = Transmitted force

$D_p$  = Pitch diameter

$n$  = angular speed

### 4. Resultant force on the shaft

Is an Additional force acting on the shaft because of the gear angle. It is calculated by the following formula.

$$F_r = \frac{F_t}{\cos \theta} \quad (25)$$

Where,

$F_r$  = Resultant force

### 5. Shear stress

Is the stress resulted from the parallel force on the system , calculated by the following formula.

$$\sigma_s = \frac{16T}{\pi D^3} \quad (26)$$

### 6. Bending stress of circular shafts

Shafts transmit power through gears and pulleys, these produce bending load in addition to torsion

$$\sigma_x = \frac{My}{I} \quad (27)$$

Where,

$\sigma_x$  = bending stress

M = calculated bending moment

Y = vertical distance away from the neutral axis

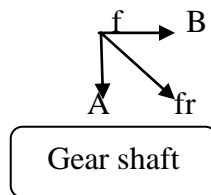
I = area moment of inertia

$$I = \frac{\pi(D^2 - d^2)}{64} \quad (28)$$

Where,

D = outside diameter

d = inside diameter



$$F = f_r \times \cos\theta \quad (29)$$

Where,

$F_r$  = Resultant force

$\theta$  = pressure angle

## 7. Twisting moment

Defined to be the algebraic sum of the moments of the applied to one side of shaft. It is calculated by the following formula.

$$M = \frac{\pi}{16} \times \tau \times d^3 \quad (30)$$

M = twisting moment

## 8. Combined maximum shear stress

Due to the complex force exerted to the system the combined maximum shear stress test is acquired

$$\tau = \left( \sigma_s^2 + \left( \frac{\sigma}{2} \right)^2 \right)^{1/2} \quad (31)$$

Where,

$\tau$  = combined maximum shear stress

### 9. Maximum normal stress

$$\sigma_e = \frac{\sigma}{2} \pm (\sigma_s^2 + \left(\frac{\sigma}{2}\right)^2)^{1/2} \quad (32)$$

Where,

$\sigma_e$  = equivalent combined normal stress

$\sigma$  = normal stress from bending or axial loads

### 10. Analysis of stress point critical section

Critical sections are the points where the minimum or maximum values of stress are calculated to

determine the where the maximum or minimum deformations of system will occur

$$\sigma_x = \frac{Mc}{I} + \frac{P}{area} \quad (33)$$

$$\sigma_x = \frac{Fl\left(\frac{d}{2}\right)}{I} + \frac{4P}{\pi d^2} \quad (34)$$

$$\tau_{xy} = \frac{Tr}{j} = \frac{16T}{\pi d^3} \quad (35)$$

Where,

$c$  = perpendicular distance from the neutral axis to the farthest point on the section

$P$  = pulling force

$F$  = applied force

$L$  = moment arm

$\tau_{xy}$  = shear stress around x, y axis's

Von misses stress is calculated to determine if the given material will yield or fracture. To find von-misses stress the following formula used is

$$\sigma_{vm} = \sqrt{(\sigma_x^2 + 3\tau_{xy}^2)} \quad (36)$$

$$\sigma_{1,2} = 0.5(\sigma_x + \sigma_y) \pm \sqrt{\frac{(\sigma_x - \sigma_y)^2}{2} + \tau_{xy}^2} \quad (37)$$

$$\tau_{max}, \tau_{min} = \pm 0.5 \sqrt{(\sigma_x)^2 + 4\tau_{xy}^2} \quad (38)$$

Where,

$\sigma_{vm}$  = von mises stress

$\sigma_x$  = stress about x axis

$\sigma_y$  = stress about y axis

$\sigma_{1,2}$  = principle stresses at certain point

$\tau_{min}$  = minimum shear stress at certain point

$\tau_{max}$  = maximum shear stress at certain point

## Appendix B

### The Properties Of Mild Steel

Property	Value	Unit
Elastic Modulus	200000	N/mm <sup>2</sup>
Poisson's Ratio	0.29	N/A
Shear Modulus	77000	N/mm <sup>2</sup>
Mass Density	7900	kg/m <sup>3</sup>
Tensile Strength	420.507	N/mm <sup>2</sup>
Yield Strength	351.571	N/mm <sup>2</sup>
Thermal Expansion Coefficient	1.5e-005	/K
Thermal Conductivity	47	W/(m·K)
Specific Heat	420	J/(kg·K)

### The Properties Of Aluminum

Property	Value	Unit
Elastic Modulus	370000	N/mm <sup>2</sup>
Poisson's Ratio	0.22	N/A
Shear Modulus	150000	N/mm <sup>2</sup>
Mass Density	3960	kg/m <sup>3</sup>
Tensile Strength	300	N/mm <sup>2</sup>
Compressive Strength	3000	N/mm <sup>2</sup>
Thermal Expansion Coefficient	7.4e-006	/K
Thermal Conductivity	30	W/(m·K)
Specific Heat	850	J/(kg·K)

### The Properties Of Stainless Steel



Property	Value	Unit
Elastic Modulus	190000	N/mm <sup>2</sup>
Poisson's Ratio	0.29	N/A
Shear Modulus	75000	N/mm <sup>2</sup>
Mass Density	8000	kg/m <sup>3</sup>
Tensile Strength	517.017	N/mm <sup>2</sup>
Yield Strength	206.807	N/mm <sup>2</sup>
Thermal Expansion Coefficient	1.8e-005	/K
Thermal Conductivity	16	W/(m·K)
Specific Heat	500	J/(kg·K)